

Analysis of the hidden-charm pentaquark states based on magnetic moment and transition magnetic moment

Fei Guo^{1,*} and Hao-Song Li^{1,2,3,4,†}

¹*School of Physics, Northwest University, Xian 710127, China*

²*Institute of Modern Physics, Northwest University, Xian 710127, China*

³*Shaanxi Key Laboratory for Theoretical Physics Frontiers, Xian 710127, China*

⁴*Peng Huanwu Center for Fundamental Theory, Xian 710127, China*

In this work, we calculate the magnetic moments of the $P_\psi^{N^0}$ states and $P_\psi^{\Delta^0}$ states with valence quark content $\bar{c}cudd$ in molecular model, diquark-diquark-antiquark model and diquark-triquark model, as well as the transition magnetic moments in the molecular model. At the same time, we also calculate magnetic moments and transition magnetic moments of $P_\psi^{\Delta^{++}}$ states and $P_\psi^{\Delta^-}$ states in the molecular model as additional products. Our results show that in the diquark-diquark-antiquark model, the magnetic moments of λ excitation state are usually larger than the magnetic moments of ρ excitation state. We find some interesting proportional relationships between the expressions of transition magnetic moments. The results provide important insights for future experimental observation of hidden-charm pentaquark states and help to distinguish their inner structures. With these efforts, our understanding of the properties for the hidden-charm pentaquark states will become more abundant.

PACS numbers:

Keywords:

I. INTRODUCTION

In the early 1960s, M. Gell-Mann and G. Zweig proposed the multiquark states beyond the conventional meson and baryon in the quark model[1, 2]. With the development of QCD, more complex quark structures are allowed theoretically. These unconventional hadrons are called exotic hadrons, such as tetraquark ($\bar{q}q\bar{q}q$) and pentaquark ($\bar{q}qqqq$). In recent years, more and more exotic hadrons states beyond the conventional quark model have been observed experimentally[3–20]. The exploration of multiquark states has entered upon a new era.

The study of pentaquark states made important progress in 2015, the LHCb collaboration observed two hidden-charm pentaquark candidates $P_\psi^N(4380)^+$ and $P_\psi^N(4450)^+$ in the $J/\psi p$ invariant mass distribution[15]. In 2019, $P_\psi^N(4450)^+$ was updated to $P_\psi^N(4440)^+$ and $P_\psi^N(4457)^+$, and a new structure $P_\psi^N(4312)^+$ was observed[16]. In this work, we adopted a new naming convention for exotic hadrons[17]. The masses and widths for these states were reported as (in units of

MeV):

$$\begin{aligned} P_\psi^N(4380)^+ &: M = 4380 \pm 8 \pm 29 \quad \Gamma = 205 \pm 18 \pm 86 \\ P_\psi^N(4440)^+ &: M = 4440.3 \pm 1.3_{-4.7}^{+4.1} \quad \Gamma = 20.6 \pm 4.9_{-10.1}^{+8.7} \\ P_\psi^N(4457)^+ &: M = 4457.3 \pm 0.6_{-1.7}^{+4.1} \quad \Gamma = 6.4 \pm 2.0_{-1.9}^{+5.7} \\ P_\psi^N(4312)^+ &: M = 4311.9 \pm 0.7_{-0.6}^{+6.8} \quad \Gamma = 9.8 \pm 2.7_{-4.5}^{+3.7} \end{aligned}$$

Recently, the research on strange hidden-charm pentaquark states ushered in new experimental progress. In 2020, the LHCb collaboration reported a strange hidden-charmed pentaquark candidate $P_{\psi_s}^\Lambda(4459)^0$ in the $\Xi_b^- \rightarrow J/\psi \Lambda K^-$ decay[18]. After considering all systematic uncertainties, its significance exceeds 3σ . In recent years, a hidden-charm pentaquark candidates $P_\psi^N(4337)^+$ [19] and a strange hidden-charm $P_{\psi_s}^\Lambda(4338)^0$ [20] were reported in 2021 and 2022 respectively. The masses and widths for these states were reported as (in units of MeV):

$$\begin{aligned} P_{\psi_s}^\Lambda(4459)^0 &: M = 4458.8 \pm 2.9_{-1.1}^{+4.7} \quad \Gamma = 17.3 \pm 6.5_{-5.7}^{+8.0} \\ P_\psi^N(4337)^+ &: M = 4337_{-4}^{+7+2} \quad \Gamma = 29_{-12-14}^{+26+14} \\ P_{\psi_s}^\Lambda(4338)^0 &: M = 4338.2 \pm 0.7 \pm 0.4 \quad \Gamma = 7.0 \pm 1.2 \pm 1.3 \end{aligned}$$

After these pentaquark states were observed, theorists proposed many models to explain their internal structures [21–44]. Theorists have obtained a good description for the pentaquark mass spectrum and de-

*Electronic address: guofei@stumail.nwu.edu.cn

†Electronic address: haosongli@nwu.edu.cn

cay patterns in the three models including molecular model[21–31], diquark-diquark-antiquark model[32–38] and diquark-triquark model[39–41]. In Ref. [45], the mass spectrum of pentaquark states in the molecular model are predicted with a phenomenological model. In Ref. [46], the author performed the research on the coupled-channel of molecular states $\Xi_c^* \bar{D}^*$, $\Xi_c' \bar{D}^*$, $\Xi_c^* \bar{D}$, $\Xi_c \bar{D}^*$, $\Xi_c' \bar{D}$, $\Lambda_c \bar{D}_s^*$, $\Xi_c \bar{D}$ and $\Lambda J/\psi$, and estimated the invariant mass spectrum by constructing potential kernel with effective Lagrangians. The mass spectrum of hidden charm pentaquarks were studied in framework of the chromomagnetic model [47].

The discovery of these hidden-charm pentaquarks $P_\psi^{N^+}(\bar{c}cuud)$ naturally leads us to speculate that other hidden-charm pentaquarks $P_\psi^{N^0}(\bar{c}cudd)$ also exists. The $P_\psi^{N^+}$ states are predicted isospin doublets with neutral partners $P_\psi^{N^0}$ states. The valence quark content of the $P_\psi^{N^0}$ states and $P_\psi^{\Delta^0}$ states is $\bar{c}cudd$, and they are closely related, so we consider these two hidden-charm pentaquark states. In order to explore more valuable information, we study the magnetic moment and transition magnetic moment of $P_\psi^{N^0}$ states and $P_\psi^{\Delta^0}$ states. The magnetic moment and transition magnetic moment provide useful clues for studying the internal structure of these exotic hadrons [48–61]. The magnetic moments, the transition magnetic moments, and the radiative decay behaviors of the of the S -wave isoscalar $\Xi_c^{(*)} \bar{D}^{(*)}$ molecular pentaquark states have been studied in Ref. [48]. In Ref. [51], the author discussed the composition of the color-flavor configurations of the pentaquark states in the molecular model, diquark-diquark-antiquark model and diquark-triquark model, and calculates the magnetic moments in these three models. In Ref. [52], the author considered P_ψ^N states as pure molecular states without flavor mixing, and it can be divided into $P_\psi^{N^+}$ states and $P_\psi^{N^0}$ states, and then calculated the magnetic moments and transition magnetic moments of the P_ψ^N states and P_ψ^{Δ} states in the molecular model.

The study of the magnetic moments and transition magnetic moments of the $P_\psi^{N^0}$ states and $P_\psi^{\Delta^0}$ states will help us understand its inner structure and search for $P_\psi^{N^0}$ states and $P_\psi^{\Delta^0}$ states in the photoproduction process. We believe that with the continuous progress of the experimental and theoretical research on the pentaquark states, the discovery of the $P_\psi^{N^0}$ states and $P_\psi^{\Delta^0}$ states will become possible in the future, which will enrich the exotic hadron family.

The organizational structure of this paper is as follows. In Sec. II, we construct the flavor wave functions in the molecular model, diquark-diquark-antiquark model and diquark-triquark model, and discuss the color configurations in these three models. In Sec. III, we calculate the magnetic moments and transition magnetic moments of the $P_\psi^{N^0}$ states and $P_\psi^{\Delta^0}$ states in the molecular model. In Sec. IV, we calculate the magnetic moments of the $P_\psi^{N^0}$ states and $P_\psi^{\Delta^0}$ states in the diquark-diquark-antiquark model. In Sec. V, we calculate the magnetic moments of the $P_\psi^{N^0}$ states and $P_\psi^{\Delta^0}$ states in the diquark-triquark model. In Sec. VI, we analyze the numerical results of magnetic moments and transition magnetic moments. In Sec. VII, we briefly summarize our work.

II. FLAVOR-COLOR WAVE FUNCTIONS OF THE HIDDEN-CHARM PENTAQUARK STATES

TABLE I: The flavor wave functions of the $P_\psi^{N^0}$ states and $P_\psi^{\Delta^0}$ states in different models, where $\{q_1 q_2\} = \sqrt{\frac{1}{2}}(q_1 q_2 + q_2 q_1)$, $[q_1 q_2] = \sqrt{\frac{1}{2}}(q_1 q_2 - q_2 q_1)$. I and I_3 are the isospin and its third component, respectively.

Molecular model ($\Sigma_c^{(*)} \bar{D}^{(*)} / \Lambda_c D^{(*)}$)			
States	Multiple	(I, I_3)	Wave function
$P_\psi^{\Delta^0}$	10_f	$(\frac{3}{2}, -\frac{1}{2})$	$\sqrt{\frac{2}{3}} \Sigma_c^{(*)+} D^{(*)-}\rangle + \sqrt{\frac{1}{3}} \Sigma_c^{(*)0} \bar{D}^{(*)0}\rangle$
$P_\psi^{N^0}$	8_{1f}	$(\frac{1}{2}, -\frac{1}{2})$	$\sqrt{\frac{1}{3}} \Sigma_c^{(*)+} D^{(*)-}\rangle - \sqrt{\frac{2}{3}} \Sigma_c^{(*)0} \bar{D}^{(*)0}\rangle$
	8_{2f}	$(\frac{1}{2}, -\frac{1}{2})$	$ \Lambda_c^+ D^{(*)-}\rangle$
Diquark-diquark-antiquark model			
$P_\psi^{\Delta^0}$	10_f	$(\frac{3}{2}, -\frac{1}{2})$	$\sqrt{\frac{2}{3}}(cd)\{ud\}\bar{c} + \sqrt{\frac{1}{3}}(cu)\{dd\}\bar{c}$
$P_\psi^{N^0}$	8_{1f}	$(\frac{1}{2}, -\frac{1}{2})$	$\sqrt{\frac{1}{3}}(cd)\{ud\}\bar{c} - \sqrt{\frac{2}{3}}(cu)\{dd\}\bar{c}$
	8_{2f}	$(\frac{1}{2}, -\frac{1}{2})$	$(cd)[ud]\bar{c}$
Diquark-triquark model			
$P_\psi^{\Delta^0}$	10_f	$(\frac{3}{2}, -\frac{1}{2})$	$\sqrt{\frac{2}{3}}(cd)(\bar{c}\{ud\}) + \sqrt{\frac{1}{3}}(cu)(\bar{c}\{dd\})$
$P_\psi^{N^0}$	8_{1f}	$(\frac{1}{2}, -\frac{1}{2})$	$\sqrt{\frac{1}{3}}(cd)(\bar{c}\{ud\}) - \sqrt{\frac{2}{3}}(cu)(\bar{c}\{dd\})$
	8_{2f}	$(\frac{1}{2}, -\frac{1}{2})$	$(cd)(\bar{c}[ud])$

In this part, we introduce the flavor-color wave functions of the hidden-charm pentaquark states in molecular model ($\bar{c}q_3)(cq_1 q_2)$, diquark-diquark-antiquark model ($cq_3)(q_1 q_2)\bar{c}$ and diquark-triquark model ($cq_3)(\bar{c}q_1 q_2)$,

where $q_{1,2,3}$ is the light quark. We construct the flavor wave functions of the pentaquark states in the $SU(3)_f$ frame. The q_1q_2 forms the $\bar{3}_f$ and 6_f flavor representation with the total spin $S = 0$ and 1 , respectively. The q_3 combines with q_1q_2 in $\bar{3}_f$ and 6_f to form the flavor representation $\bar{3}_f \otimes 3_f = 1_f \oplus 8_{2f}$ and $6_f \otimes 3_f = 10_f \oplus 8_{1f}$, respectively. After inserting c , \bar{c} and the Clebsch-Gordan coefficients, we obtained the flavor wave functions in the molecular model with the configuration $(\bar{c}q_3)(cq_1q_2)$. The same method is applied to the other configurations $(cq_3)(\bar{c}q_1q_2)$ and $(cq_3)(q_1q_2)\bar{c}$. Here, the flavor wave function in the 1_f flavor representation is $\sqrt{\frac{1}{3}}\{(\bar{c}d)(c[us]) - (\bar{c}u)(c[ds]) + (\bar{c}s)(c[ud])\}$, which includes charm, up, down and strange quarks, so we did not consider the 1_f flavor representation. In our work, we study the hidden-charm pentaquark states with valence quark content $\bar{c}cudd$, including the $P_\psi^{N^0}$ states with isospin $I = \frac{1}{2}$ and $P_\psi^{\Delta^0}$ states with isospin $I = \frac{3}{2}$. The $P_\psi^{N^0}$ states and $P_\psi^{\Delta^0}$ states correspond to 8_f and 10_f flavor representations, respectively. Therefore, we list the flavor wave functions of the $P_\psi^{N^0}$ states and $P_\psi^{\Delta^0}$ states in the molecular model, diquark-diquark-antiquark model and diquark-triquark model in Table I. When calculating the magnetic moments in the three models, we simultaneously consider the S -wave and P -wave states.

The color confinement hypothesis implies that all hadrons must be color singlets which means that they do not change in the color $SU(3)$ space. We briefly introduce the color configurations of the hidden-charm pentaquark states in three models.

1. Molecular model $(\bar{c}q_3)(cq_1q_2)$: The hidden-charm pentaquark states in the molecular model $(\bar{c}q_3)(cq_1q_2)$ are composed of two clusters of meson and baryon. As a molecular state, $\bar{c}q_3$ and cq_1q_2 are in the color singlet. The color representation of $(\bar{c}q_3)$ cluster tends to be $\bar{3}_c \otimes 3_c = 1_c \oplus 8_c$, the color representation of (cq_1q_2) cluster tends to be $3_c \otimes (3_c \otimes 3_c) = 3_c \otimes (\bar{3}_c \oplus 6_c) = (1_c \oplus 8_{2c}) \oplus (8_{1c} \oplus 10_c)$.

2. Diquark-diquark-antiquark model $(cq_3)(q_1q_2)\bar{c}$: In this model, diquark (cq_3) and diquark (q_1q_2) are both antisymmetric $\bar{3}_c$ color representation, and $(\bar{3}_c \otimes \bar{3}_c)$ prefers to form 3_c . The \bar{c} is also on the $\bar{3}_c$ color representation, using $(\bar{3}_c \otimes \bar{3}_c) \otimes \bar{3}_c = 3_c \otimes \bar{3}_c$ obtain the color singlet representation of the diquark-diquark-antiquark model.

3. Diquark-triquark model $(cq_3)(\bar{c}q_1q_2)$: In the diquark-triquark model, triquark $(\bar{c}q_1q_2)$ is symmetric 3_c color representation, and diquark (cq_3) is antisymmetric $\bar{3}_c$ color representation. So we have $3_c \otimes \bar{3}_c$ obtain a color

singlet.

III. MAGNETIC MOMENTS AND TRANSITION MAGNETIC MOMENTS OF THE $P_\psi^{N^0}$ STATES AND $P_\psi^{\Delta^0}$ STATES IN THE MOLECULAR MODEL

The magnetic moment of a compound system is the sum of its constituent magnetic moments, including spin magnetic moment and orbital magnetic moment,

$$\vec{\mu} = \vec{\mu}_{spin} + \vec{\mu}_{orbital} = \sum_i (g_i \vec{S}_i + \vec{l}_i) \mu_i, \quad (1)$$

where g_i is the g factor of i -th constituent, \vec{S}_i is the spin of the i -th constituent and μ_i is the magneton of the i -th constituent,

$$\mu_i = \frac{q_i}{2m_i}. \quad (2)$$

In the above expression, q_i and m_i as the charge and mass of the i -th constituent, respectively. In the molecular model, the constituents of spin magnetic moment are baryons and mesons.

The total magnetic moment of hidden-charm pentaquark states in the molecular model $(\bar{c}q_3)(cq_1q_2)$ includes the sum of the meson spin magnetic moment, the baryon spin magnetic moment and the orbital magnetic moment

$$\vec{\mu} = g_m \mu_m \vec{S}_m + g_b \mu_b \vec{S}_b + \mu_l \vec{l}, \quad (3)$$

$$\mu_l = \frac{m_b \mu_m + m_m \mu_b}{m_m + m_b}, \quad (4)$$

where μ_l is the orbital magnetic moment between the two hadrons. The subscripts m and b represent meson and baryon, respectively. We use the masses of mesons and baryons from Particle Data Group [62]. The magnetic moment formula of hidden-charm pentaquark states $(\bar{c}q_3)(cq_1q_2)$ in the molecular model is

$$\begin{aligned} \mu &= \left\langle \psi \left| g_m \mu_m \vec{S}_m + g_b \mu_b \vec{S}_b + \mu_l \vec{l} \right| \psi \right\rangle \\ &= \sum_{l_z, S_z} \langle l_l z, S S_z | J J_z \rangle^2 \left\{ \mu_l l_z + \sum_{S'_b} \left\langle S_b S'_b, S_m (S_z \right. \right. \\ &\quad \left. \left. - S'_b) | S S_z \right\rangle^2 \left[(S_z - S'_b) (\mu_{\bar{c}} + \mu_{q_3}) \right. \right. \\ &\quad \left. \left. + \sum_{S'_c, S'_{12}} \langle S_c S'_c, S_{12} S'_{12} | S_b S'_b \rangle^2 (g_c \mu_c S'_c + S'_{12} (\mu_{q_1} \right. \right. \\ &\quad \left. \left. + \mu_{q_2})) \right] \right\}, \quad (5) \end{aligned}$$

TABLE II: The magnetic moments of the $P_\psi^{N^0}$ states in the molecular model with the 8_{1f} and 8_{2f} flavor representation. The $J_1^{P_1} \otimes J_2^{P_2} \otimes J_3^{P_3}$ are corresponding to the angular momentum and parity of baryon, meson and orbital, respectively. The $\mu_{l(\text{baryon}/\text{meson})}$ represents the orbital excitation between corresponding hadrons. The unit is the nuclear magnetic moment μ_N .

$ \Lambda_c^+ D^{(*)-}\rangle$				
J^P	$^{2s+1}L_J$	$J_1^{P_1} \otimes J_2^{P_2} \otimes J_3^{P_3}$	Expressions	Results
$\frac{1}{2}^-$	$^2S_{\frac{1}{2}}$	$\frac{1}{2}^+ \otimes 0^- \otimes 0^+$	μ_c	0.403
		$\frac{1}{2}^+ \otimes 1^- \otimes 0^+$	$\frac{1}{3}(-4\mu_c + 2\mu_d)$	-1.035
$\frac{3}{2}^-$	$^4S_{\frac{3}{2}}$	$\frac{1}{2}^+ \otimes 1^- \otimes 0^+$	μ_d	-0.947
$\frac{1}{2}^+$	$^2P_{\frac{1}{2}}$	$\frac{1}{2}^+ \otimes 0^- \otimes 1^-$	$\frac{1}{3}(-\mu_c + 2\mu_{l(\Lambda_c^+/D^-)})$	-0.196
		$(\frac{1}{2}^+ \otimes 1^-)_{\frac{1}{2}} \otimes 1^-$	$\frac{1}{9}(3\mu_c - 2\mu_d + 6\mu_{l(\Lambda_c^+/D^{*-})})$	0.750
	$^4P_{\frac{1}{2}}$	$(\frac{1}{2}^+ \otimes 1^-)_{\frac{3}{2}} \otimes 1^-$	$\frac{1}{9}(5\mu_d - 3\mu_{l(\Lambda_c^+/D^{*-})})$	-0.507
$\frac{3}{2}^+$	$^2P_{\frac{3}{2}}$	$\frac{1}{2}^+ \otimes 0^- \otimes 1^-$	$\mu_c + \mu_{l(\Lambda_c^+/D^-)}$	0.311
		$(\frac{1}{2}^+ \otimes 1^-)_{\frac{1}{2}} \otimes 1^-$	$\frac{1}{3}(-3\mu_c + 2\mu_d + 3\mu_{l(\Lambda_c^+/D^{*-})})$	-1.092
	$^4P_{\frac{3}{2}}$	$(\frac{1}{2}^+ \otimes 1^-)_{\frac{3}{2}} \otimes 1^-$	$\frac{1}{15}(11\mu_d + 6\mu_{l(\Lambda_c^+/D^{*-})})$	-0.718
$\frac{5}{2}^+$	$^4P_{\frac{5}{2}}$	$\frac{1}{2}^+ \otimes 1^- \otimes 1^-$	$\mu_d + \mu_{l(\Lambda_c^+/D^{*-})}$	-1.004
$\sqrt{\frac{1}{3}} \Sigma_c^{(*)+}D^{(*)-}\rangle - \sqrt{\frac{2}{3}} \Sigma_c^{(*)0}\bar{D}^{(*)0}\rangle$				
J^P	$^{2s+1}L_J$	$J_1^{P_1} \otimes J_2^{P_2} \otimes J_3^{P_3}$	Expressions	Results
$\frac{1}{2}^-$	$^2S_{\frac{1}{2}}$	$\frac{1}{2}^+ \otimes 0^- \otimes 0^+$	$\frac{1}{9}(2\mu_u + 10\mu_d - 3\mu_c)$	-0.766
		$\frac{1}{2}^+ \otimes 1^- \otimes 0^+$	$\frac{1}{27}(10\mu_u - 4\mu_d - 15\mu_c)$	0.618
		$\frac{3}{2}^+ \otimes 1^- \otimes 0^+$	$\frac{1}{27}(-\mu_u + 22\mu_d + 24\mu_c)$	-0.483
$\frac{3}{2}^-$	$^4S_{\frac{3}{2}}$	$\frac{1}{2}^+ \otimes 1^- \otimes 0^+$	$\frac{1}{9}(8\mu_u + 13\mu_d - 12\mu_c)$	-0.222
		$\frac{3}{2}^+ \otimes 0^- \otimes 0^+$	$\frac{1}{3}(\mu_u + 5\mu_d + 3\mu_c)$	-0.544
		$\frac{3}{2}^+ \otimes 1^- \otimes 0^+$	$\frac{1}{45}(23\mu_u + 61\mu_d + 15\mu_c)$	-0.181
$\frac{5}{2}^-$	$^6S_{\frac{5}{2}}$	$\frac{3}{2}^+ \otimes 1^- \otimes 0^+$	$\mu_u + 2\mu_d$	0
$\frac{1}{2}^+$	$^2P_{\frac{1}{2}}$	$\frac{1}{2}^+ \otimes 0^- \otimes 1^-$	$\frac{1}{27}(-2\mu_u - 10\mu_d + 3\mu_c + 6\mu_{l(\Sigma_c^+/D^-)} + 12\mu_{l(\Sigma_c^0/\bar{D}^0)})$	0.229
		$(\frac{1}{2}^+ \otimes 1^-)_{\frac{1}{2}} \otimes 1^-$	$\frac{1}{81}(-10\mu_u + 4\mu_d + 15\mu_c + 18\mu_{l(\Sigma_c^+/D^{*-})} + 36\mu_{l(\Sigma_c^0/\bar{D}^0)})$	-0.225
	$^4P_{\frac{1}{2}}$	$(\frac{1}{2}^+ \otimes 1^-)_{\frac{3}{2}} \otimes 1^-$	$\frac{1}{81}(40\mu_u + 65\mu_d - 60\mu_c - 9\mu_{l(\Sigma_c^+/D^{*-})} - 18\mu_{l(\Sigma_c^0/\bar{D}^0)})$	-0.114
		$\frac{3}{2}^+ \otimes 0^- \otimes 1^-$	$\frac{1}{27}(5\mu_u + 25\mu_d + 15\mu_c - 3\mu_{l(\Sigma_c^{*+}/D^-)} - 6\mu_{l(\Sigma_c^{*0}/\bar{D}^0)})$	-0.289
$^2P_{\frac{1}{2}}$	$(\frac{3}{2}^+ \otimes 1^-)_{\frac{1}{2}} \otimes 1^-$	$\frac{1}{81}(\mu_u - 22\mu_d - 24\mu_c + 18\mu_{l(\Sigma_c^{*+}/D^{*-})} + 36\mu_{l(\Sigma_c^0/\bar{D}^0)})$	0.140	
	$^4P_{\frac{1}{2}}$	$(\frac{3}{2}^+ \otimes 1^-)_{\frac{3}{2}} \otimes 1^-$	$\frac{1}{81}(23\mu_u + 61\mu_d + 15\mu_c - 9\mu_{l(\Sigma_c^{*+}/D^{*-})} - 18\mu_{l(\Sigma_c^0/\bar{D}^0)})$	-0.090
$\frac{3}{2}^+$	$^2P_{\frac{3}{2}}$	$\frac{1}{2}^+ \otimes 0^- \otimes 1^-$	$\frac{1}{9}(2\mu_u + 10\mu_d - 3\mu_c + 3\mu_{l(\Sigma_c^+/D^-)} + 6\mu_{l(\Sigma_c^0/\bar{D}^0)})$	-0.806
		$(\frac{1}{2}^+ \otimes 1^-)_{\frac{1}{2}} \otimes 1^-$	$\frac{1}{27}(10\mu_u - 4\mu_d - 15\mu_c + 9\mu_{l(\Sigma_c^+/D^{*-})} + 18\mu_{l(\Sigma_c^0/\bar{D}^0)})$	0.590
	$^4P_{\frac{3}{2}}$	$(\frac{1}{2}^+ \otimes 1^-)_{\frac{3}{2}} \otimes 1^-$	$\frac{1}{135}(88\mu_u + 143\mu_d - 132\mu_c + 18\mu_{l(\Sigma_c^+/D^{*-})} + 36\mu_{l(\Sigma_c^0/\bar{D}^0)})$	-0.174
		$\frac{3}{2}^+ \otimes 0^- \otimes 1^-$	$\frac{1}{45}(11\mu_u + 55\mu_d + 33\mu_c + 6\mu_{l(\Sigma_c^{*+}/D^-)} + 12\mu_{l(\Sigma_c^0/\bar{D}^0)})$	-0.415
	$^2P_{\frac{3}{2}}$	$(\frac{3}{2}^+ \otimes 1^-)_{\frac{1}{2}} \otimes 1^-$	$\frac{1}{27}(-\mu_u + 22\mu_d + 24\mu_c + 9\mu_{l(\Sigma_c^{*+}/D^{*-})} + 18\mu_{l(\Sigma_c^0/\bar{D}^0)})$	-0.515
$^4P_{\frac{3}{2}}$	$(\frac{3}{2}^+ \otimes 1^-)_{\frac{3}{2}} \otimes 1^-$	$\frac{1}{675}(253\mu_u + 671\mu_d + 165\mu_c + 90\mu_{l(\Sigma_c^{*+}/D^{*-})} + 180\mu_{l(\Sigma_c^0/\bar{D}^0)})$	-0.146	
$^6P_{\frac{3}{2}}$	$(\frac{3}{2}^+ \otimes 1^-)_{\frac{5}{2}} \otimes 1^-$	$\frac{1}{75}(63\mu_u + 126\mu_d - 15\mu_{l(\Sigma_c^{*+}/D^{*-})} - 30\mu_{l(\Sigma_c^0/\bar{D}^0)})$	0.019	
$\frac{5}{2}^+$	$^4P_{\frac{5}{2}}$	$\frac{1}{2}^+ \otimes 1^- \otimes 1^-$	$\frac{1}{9}(8\mu_u + 13\mu_d - 12\mu_c + 3\mu_{l(\Sigma_c^+/D^{*-})} + 6\mu_{l(\Sigma_c^0/\bar{D}^0)})$	-0.125
		$\frac{3}{2}^+ \otimes 0^- \otimes 1^-$	$\frac{1}{3}(\mu_u + 5\mu_d + 3\mu_c + \mu_{l(\Sigma_c^{*+}/D^-)} + 2\mu_{l(\Sigma_c^0/\bar{D}^0)})$	-0.584
		$(\frac{3}{2}^+ \otimes 1^-)_{\frac{3}{2}} \otimes 1^-$	$\frac{1}{45}(23\mu_u + 61\mu_d + 15\mu_c + 15\mu_{l(\Sigma_c^{*+}/D^{*-})} + 30\mu_{l(\Sigma_c^0/\bar{D}^0)})$	-0.213
$^6P_{\frac{5}{2}}$	$(\frac{3}{2}^+ \otimes 1^-)_{\frac{5}{2}} \otimes 1^-$	$\frac{1}{105}(93\mu_u + 186\mu_d + 10\mu_{l(\Sigma_c^{*+}/D^{*-})} + 20\mu_{l(\Sigma_c^0/\bar{D}^0)})$	-0.009	
$\frac{7}{2}^+$	$^6P_{\frac{7}{2}}$	$\frac{3}{2}^+ \otimes 1^- \otimes 1^-$	$\frac{1}{3}(3\mu_u + 6\mu_d + \mu_{l(\Sigma_c^{*+}/D^{*-})} + 2\mu_{l(\Sigma_c^0/\bar{D}^0)})$	-0.031

TABLE III: The magnetic moments of the $P_\psi^{\Lambda^0}$ states in the molecular model with the 10_f flavor representation. The $J_1^{P_1} \otimes J_2^{P_2} \otimes J_3^{P_3}$ are corresponding to the angular momentum and parity of baryon, meson and orbital, respectively. The $\mu_{l(\text{baryon/meson})}$ represents the orbital excitation between corresponding hadrons. The unit is the nuclear magnetic moment μ_N .

$\sqrt{\frac{2}{3}} \Sigma_c^{(*)+} D^{(*)-}\rangle + \sqrt{\frac{1}{3}} \Sigma_c^{(*)0} \bar{D}^{(*)0}\rangle$				
J^P	$^{2s+1}L_J$	$J_1^{P_1} \otimes J_2^{P_2} \otimes J_3^{P_3}$	Expressions	Results
$\frac{1}{2}^-$	$^2S_{\frac{1}{2}}$	$\frac{1}{2}^+ \otimes 0^- \otimes 0^+$	$\frac{1}{9} (4\mu_u + 8\mu_d - 3\mu_c)$	-0.134
		$\frac{1}{2}^+ \otimes 1^- \otimes 0^+$	$\frac{1}{27} (2\mu_u + 4\mu_d - 15\mu_c)$	-0.224
		$\frac{3}{2}^+ \otimes 1^- \otimes 0^+$	$\frac{1}{27} (7\mu_u + 14\mu_d + 24\mu_c)$	0.359
$\frac{3}{2}^-$	$^4S_{\frac{3}{2}}$	$\frac{1}{2}^+ \otimes 1^- \otimes 0^+$	$\frac{1}{9} (7\mu_u + 14\mu_d - 12\mu_c)$	-0.538
		$\frac{3}{2}^+ \otimes 0^- \otimes 0^+$	$\frac{1}{3} (2\mu_u + 4\mu_d + 3\mu_c)$	0.403
		$\frac{3}{2}^+ \otimes 1^- \otimes 0^+$	$\frac{1}{45} (28\mu_u + 56\mu_d + 15\mu_c)$	0.134
$\frac{5}{2}^-$	$^6S_{\frac{5}{2}}$	$\frac{3}{2}^+ \otimes 1^- \otimes 0^+$	$\mu_u + 2\mu_d$	0
$\frac{1}{2}^+$	$^2P_{\frac{1}{2}}$	$\frac{1}{2}^+ \otimes 0^- \otimes 1^-$	$\frac{1}{27} (-4\mu_u - 8\mu_d + 3\mu_c + 12\mu_{l(\Sigma_c^+ / D^-)} + 6\mu_{l(\Sigma_c^0 / \bar{D}^0)})$	-0.009
		$(\frac{1}{2}^+ \otimes 1^-)_{\frac{1}{2}} \otimes 1^-$	$\frac{1}{81} (-2\mu_u - 4\mu_d + 15\mu_c + 36\mu_{l(\Sigma_c^+ / D^{*-})} + 18\mu_{l(\Sigma_c^0 / \bar{D}^0)})$	0.037
	$^4P_{\frac{1}{2}}$	$(\frac{1}{2}^+ \otimes 1^-)_{\frac{3}{2}} \otimes 1^-$	$\frac{1}{81} (35\mu_u + 70\mu_d - 60\mu_c - 18\mu_{l(\Sigma_c^+ / D^{*-})} - 9\mu_{l(\Sigma_c^0 / \bar{D}^0)})$	-0.280
		$\frac{3}{2}^+ \otimes 0^- \otimes 1^-$	$\frac{1}{27} (10\mu_u + 20\mu_d + 15\mu_c - 6\mu_{l(\Sigma_c^{*+} / D^-)} - 3\mu_{l(\Sigma_c^{*0} / \bar{D}^0)})$	0.251
	$^2P_{\frac{1}{2}}$	$(\frac{3}{2}^+ \otimes 1^-)_{\frac{1}{2}} \otimes 1^-$	$\frac{1}{81} (-7\mu_u - 14\mu_d - 24\mu_c + 36\mu_{l(\Sigma_c^{*+} / D^{*-})} + 18\mu_{l(\Sigma_c^{*0} / \bar{D}^0)})$	-0.161
$^4P_{\frac{1}{2}}$	$(\frac{3}{2}^+ \otimes 1^-)_{\frac{3}{2}} \otimes 1^-$	$\frac{1}{81} (28\mu_u + 56\mu_d + 15\mu_c - 18\mu_{l(\Sigma_c^{*+} / D^{*-})} - 9\mu_{l(\Sigma_c^{*0} / \bar{D}^0)})$	0.096	
$\frac{3}{2}^+$	$^2P_{\frac{3}{2}}$	$\frac{1}{2}^+ \otimes 0^- \otimes 1^-$	$\frac{1}{9} (4\mu_u + 8\mu_d - 3\mu_c + 6\mu_{l(\Sigma_c^+ / D^-)} + 3\mu_{l(\Sigma_c^0 / \bar{D}^0)})$	-0.214
		$(\frac{1}{2}^+ \otimes 1^-)_{\frac{1}{2}} \otimes 1^-$	$\frac{1}{27} (2\mu_u + 4\mu_d - 15\mu_c + 18\mu_{l(\Sigma_c^+ / D^{*-})} + 9\mu_{l(\Sigma_c^0 / \bar{D}^0)})$	-0.281
	$^4P_{\frac{3}{2}}$	$(\frac{1}{2}^+ \otimes 1^-)_{\frac{3}{2}} \otimes 1^-$	$\frac{1}{135} (77\mu_u + 154\mu_d - 132\mu_c + 36\mu_{l(\Sigma_c^+ / D^{*-})} + 18\mu_{l(\Sigma_c^0 / \bar{D}^0)})$	-0.417
		$\frac{3}{2}^+ \otimes 0^- \otimes 1^-$	$\frac{1}{45} (22\mu_u + 44\mu_d + 33\mu_c + 12\mu_{l(\Sigma_c^{*+} / D^-)} + 6\mu_{l(\Sigma_c^{*0} / \bar{D}^0)})$	0.264
	$^2P_{\frac{3}{2}}$	$(\frac{3}{2}^+ \otimes 1^-)_{\frac{1}{2}} \otimes 1^-$	$\frac{1}{27} (7\mu_u + 14\mu_d + 24\mu_c + 18\mu_{l(\Sigma_c^{*+} / D^{*-})} + 9\mu_{l(\Sigma_c^{*0} / \bar{D}^0)})$	0.296
	$^4P_{\frac{3}{2}}$	$(\frac{3}{2}^+ \otimes 1^-)_{\frac{3}{2}} \otimes 1^-$	$\frac{1}{675} (308\mu_u + 616\mu_d + 165\mu_c + 180\mu_{l(\Sigma_c^{*+} / D^{*-})} + 90\mu_{l(\Sigma_c^{*0} / \bar{D}^0)})$	0.074
$^6P_{\frac{3}{2}}$	$(\frac{3}{2}^+ \otimes 1^-)_{\frac{5}{2}} \otimes 1^-$	$\frac{1}{75} (63\mu_u + 126\mu_d - 30\mu_{l(\Sigma_c^{*+} / D^{*-})} - 15\mu_{l(\Sigma_c^{*0} / \bar{D}^0)})$	0.038	
$\frac{5}{2}^+$	$^4P_{\frac{5}{2}}$	$\frac{1}{2}^+ \otimes 1^- \otimes 1^-$	$\frac{1}{9} (7\mu_u + 14\mu_d - 12\mu_c + 6\mu_{l(\Sigma_c^+ / D^{*-})} + 3\mu_{l(\Sigma_c^0 / \bar{D}^0)})$	-0.532
		$\frac{3}{2}^+ \otimes 0^- \otimes 1^-$	$\frac{1}{3} (2\mu_u + 4\mu_d + 3\mu_c + 2\mu_{l(\Sigma_c^{*+} / D^-)} + \mu_{l(\Sigma_c^{*0} / \bar{D}^0)})$	0.323
		$(\frac{3}{2}^+ \otimes 1^-)_{\frac{3}{2}} \otimes 1^-$	$\frac{1}{45} (28\mu_u + 56\mu_d + 15\mu_c + 30\mu_{l(\Sigma_c^{*+} / D^{*-})} + 15\mu_{l(\Sigma_c^{*0} / \bar{D}^0)})$	0.072
	$^6P_{\frac{5}{2}}$	$(\frac{3}{2}^+ \otimes 1^-)_{\frac{5}{2}} \otimes 1^-$	$\frac{1}{105} (93\mu_u + 186\mu_d + 20\mu_{l(\Sigma_c^{*+} / D^{*-})} + 10\mu_{l(\Sigma_c^{*0} / \bar{D}^0)})$	-0.018
$\frac{7}{2}^+$	$^6P_{\frac{7}{2}}$	$\frac{3}{2}^+ \otimes 1^- \otimes 1^-$	$\frac{1}{3} (3\mu_u + 6\mu_d + 2\mu_{l(\Sigma_c^{*+} / D^{*-})} + \mu_{l(\Sigma_c^{*0} / \bar{D}^0)})$	-0.063

where ψ represents the flavor wave function in molecular model in Table I, S_{12} and S'_{12} are the spin and its third componen of the diquark (q_1q_2) inside the baryon (cq_1q_2). S is the spin of pentaquark state. J is the total angular momentum of pentaquark state. S_c and S'_c are spin and third component of quark c . S_z, S'_b and l_z are the spin third component of the pentaquark state, the baryon, and the orbital excitation, respectively. In the generated table, $\mu_{\bar{c}}$ did not appear in these pentaquark state magnetic moment expressions because the relationship $\mu_c = -\mu_{\bar{c}}$ can simplify these expressions.

We take $J^P = \frac{1}{2}^- (\frac{1}{2}^+ \otimes 0^- \otimes 0^+)$ of the $\Sigma_c \bar{D}$ molecular state with the 8_{1f} flavor representation as an example. The $J_1^{P_1} \otimes J_2^{P_2} \otimes J_3^{P_3}$ are corresponding to the angular momentum and parity of baryon, meson and orbital, respectively. According to Table I, the flavor wave function can be written as

$$\begin{aligned} \psi_{\Sigma_c \bar{D}} &= \sqrt{\frac{1}{3}} |\Sigma_c^+ D^- \rangle - \sqrt{\frac{2}{3}} |\Sigma_c^0 \bar{D}^0 \rangle \\ &= \sqrt{\frac{1}{3}} (c\{ud\})(\bar{c}d) - \sqrt{\frac{2}{3}} (c\{dd\})(\bar{c}u). \end{aligned} \quad (6)$$

We obtained the magnetic moment expression

$$\begin{aligned} \mu_{\Sigma_c \bar{D}} &= \langle \psi_{\Sigma_c \bar{D}} | g_m \mu_m \vec{S}_m + g_b \mu_b \vec{S}_b + \mu_l \vec{l} | \psi_{\Sigma_c \bar{D}} \rangle \\ &= \langle 00, \frac{1}{2} \frac{1}{2} | \frac{1}{2} \frac{1}{2} \rangle^2 \left[\langle \frac{1}{2} \frac{1}{2}, 00 | \frac{1}{2} \frac{1}{2} \rangle^2 (\langle \frac{1}{2} \frac{1}{2}, 10 | \frac{1}{2} \frac{1}{2} \rangle^2 \mu_c \right. \\ &\quad \left. + \langle \frac{1}{2} - \frac{1}{2}, 11 | \frac{1}{2} \frac{1}{2} \rangle^2 (-\mu_c + \frac{1}{3} \mu_u + \frac{5}{3} \mu_d) \right] \\ &= \frac{1}{9} (2\mu_u + 10\mu_d - 3\mu_c). \end{aligned} \quad (7)$$

The magnetic moments of hidden-charm pentaquark states with isospin $(I, I_3) = (\frac{1}{2}, -\frac{1}{2})$ and $(I, I_3) = (\frac{3}{2}, -\frac{1}{2})$ in the molecular model are collected in Table II and Table III respectively. In this work, we use the following constituent quark masses [51],

$$m_u = m_d = 0.33 \text{ GeV}, m_c = 1.55 \text{ GeV}. \quad (8)$$

When we express transition magnetic moments of hidden-charm pentaquark states in the molecular model, we need the magnetic moments and the transition magnetic moments of baryon $\Sigma_c^{(*)}$ and meson $\bar{D}^{(*)}$. Since the experimental values of the magnetic moments of baryon $\Sigma_c^{(*)}$ and meson $\bar{D}^{(*)}$ are still absent, we calculate their magnetic moments and transition magnetic moments. Our numerical results are consistent with the results of other theoretical works [48–50]. We take the baryon Σ_c^+ as an example to illustrate how to obtain the magnetic moments of conventional mesons and baryons. Similar to calculating the magnetic moments of pentaquarks,

the magnetic moments of baryon with the configuration (cq_1q_2) is

$$\begin{aligned} \mu_b &= \langle \psi_b | g_b \mu_b \vec{S}_b | \psi_b \rangle \\ &= \langle \frac{1}{2} \frac{1}{2}, S_{12}(S'_b - \frac{1}{2}) | S_b S'_b \rangle^2 [\mu_c + (S'_b - \frac{1}{2})(\mu_{q_1} \\ &\quad + \mu_{q_2})] + \langle \frac{1}{2} - \frac{1}{2}, S_{12}(S'_b + \frac{1}{2}) | S_b S'_b \rangle^2 [-\mu_c \\ &\quad + (S'_b + \frac{1}{2})(\mu_{q_1} + \mu_{q_2})], \end{aligned} \quad (9)$$

where S_b is the spin of barons, S'_b is the third component of the spin of baryon, S_{12} is the spin of the diquark (q_1q_2) inside baryon (cq_1q_2). ψ_b represents flavor wave function of baryon.

We obtion the magnetic moment expression of the baryon Σ_c^+ ,

$$\begin{aligned} \mu_{\Sigma_c^+} &= \langle \psi_{\Sigma_c^+} | g_b \mu_b \vec{S}_b | \psi_{\Sigma_c^+} \rangle \\ &= \langle \frac{1}{2} \frac{1}{2}, 10 | \frac{1}{2} \frac{1}{2} \rangle^2 \mu_c + \langle \frac{1}{2} - \frac{1}{2}, 11 | \frac{1}{2} \frac{1}{2} \rangle^2 (-\mu_c + \mu_u + \mu_d) \\ &= \frac{2}{3} \mu_u + \frac{2}{3} \mu_d - \frac{1}{3} \mu_c. \end{aligned} \quad (10)$$

Similarly to the solution procedure of the magnetic moment of the baryon Σ_c^+ , we obtion the expressions of magnetic moments of the S -wave charmed baryon $\Sigma_c^{(*)}$, Λ_c and the S -wave anti-charmed meson $\bar{D}^{(*)}$ in Table IV.

TABLE IV: Magnetic moments of the S -wave charmed baryon $\Sigma_c^{(*)}$, Λ_c and the S -wave anti-charmed meson $\bar{D}^{(*)}$. Here, the magnetic moment of the S -wave anti-charmed meson \bar{D} is zero. The unit is the nuclear magnetic moment μ_N .

Hadrons	$I(J^P)$	Expressions	Results [48]	[49]	[50]
$\mu_{\Sigma_c^{*+}}$	$1(\frac{1}{2}^+)$	$\frac{4}{3}\mu_u - \frac{1}{3}\mu_c$	2.392	2.357	2.130
$\mu_{\Sigma_c^+}$		$\frac{2}{3}\mu_u + \frac{2}{3}\mu_d - \frac{1}{3}\mu_c$	0.497	0.496	0.410
$\mu_{\Sigma_c^0}$		$\frac{4}{3}\mu_d - \frac{1}{3}\mu_c$	-1.398	-1.365	-1.310
$\mu_{\Lambda_c^+}$	$0(\frac{1}{2}^+)$	μ_c	0.403		
$\mu_{\Sigma_c^{*++}}$	$1(\frac{3}{2}^+)$	$2\mu_u + \mu_c$	4.193	4.094	4.070
$\mu_{\Sigma_c^{*+}}$		$\mu_u + \mu_d + \mu_c$	1.351	1.302	1.390
$\mu_{\Sigma_c^{*0}}$		$2\mu_d + \mu_c$	-1.492	-1.490	-1.290
$\mu_{D^{*-}}$	$\frac{1}{2}(1^-)$	$\mu_d + \mu_{\bar{c}}$	-1.351	-1.303	
$\mu_{\bar{D}^{*0}}$		$\mu_u + \mu_{\bar{c}}$	1.492	1.489	

We calculate the transition magnetic moments of baryon $\Sigma_c^{(*)}$ and meson $\bar{D}^{(*)}$. The transition magnetic moment is obtained by the third component of the magnetic moment operator $\vec{\mu}_z$ acting on the hadron wave function [54],

$$\mu_{H \rightarrow H'} = \langle J_{H'} | J_z | \vec{\mu}_z | J_H, J_z \rangle^{J_z = \text{Min}[J_H, J_{H'}]}. \quad (11)$$

Here, H and H' are the corresponding wave functions of the initial and final states of the investigated hadronic state, respectively. We use the the maximum spin third component of the lowest state to discuss the transition magnetic moment between pentaquark states. For instance, we discuss the transition magnetic moment of the $\bar{D}^{*0} \rightarrow \bar{D}^0\gamma$ process. We construct the flavor-spin wave functions of mesons \bar{D}^{*0} and \bar{D}^0 as

$$\phi_{\bar{D}^{*0}}^{S=1; S_3=0} = \frac{1}{\sqrt{2}}|\bar{c}u\rangle|\uparrow\downarrow + \downarrow\uparrow\rangle, \quad (12)$$

$$\phi_{\bar{D}^0}^{S=0; S_3=0} = \frac{1}{\sqrt{2}}|\bar{c}u\rangle|\uparrow\downarrow - \downarrow\uparrow\rangle. \quad (13)$$

The transition magnetic moment of the $\bar{D}^{*0} \rightarrow \bar{D}^0\gamma$ process is

$$\begin{aligned} \mu_{\bar{D}^{*0} \rightarrow \bar{D}^0} &= \langle \phi_{\bar{D}^0}^{S=0; S_3=0} | \hat{\mu}_z | \phi_{\bar{D}^{*0}}^{S=1; S_3=0} \rangle \\ &= \left\langle \frac{\bar{c}u \uparrow\downarrow - \bar{c}u \downarrow\uparrow}{\sqrt{2}} \left| \hat{\mu}_z \right| \frac{\bar{c}u \uparrow\downarrow + \bar{c}u \downarrow\uparrow}{\sqrt{2}} \right\rangle \\ &= \mu_{\bar{c}} - \mu_u. \end{aligned} \quad (14)$$

In Table V, we present the expressions and numerical results of the transition magnetic moments of the S -wave charmed baryons $\Sigma_c^{(*)}$ and the S -wave anti-charmed mesons $\bar{D}^{(*)}$.

TABLE V: Transition magnetic moments of the S -wave charmed baryons $\Sigma_c^{(*)}$ and the S -wave anti-charmed mesons $\bar{D}^{(*)}$. The unit is the nuclear magnetic moment μ_N .

Decay modes	Expressions	Results	[48]	[49]
$\Sigma_c^{*++} \rightarrow \Sigma_c^{++}\gamma$	$\frac{2\sqrt{2}}{3}(\mu_u - \mu_c)$	1.406		1.404
$\Sigma_c^{*+} \rightarrow \Sigma_c^+\gamma$	$\frac{\sqrt{2}}{3}(\mu_u + \mu_d - 2\mu_c)$	0.066		0.088
$\Sigma_c^{*0} \rightarrow \Sigma_c^0\gamma$	$\frac{2\sqrt{2}}{3}(\mu_d - \mu_c)$	-1.274		-1.228
$\bar{D}^{*0} \rightarrow \bar{D}^0\gamma$	$-\mu_u + \mu_{\bar{c}}$	-2.298	-2.234	
$D^{*-} \rightarrow D^-\gamma$	$-\mu_d + \mu_{\bar{c}}$	0.544	0.588	

Next, we calculate the transition magnetic moments of S -wave hidden-charm pentaquark $P_\psi^{N^0}$ states and $P_\psi^{\Delta^0}$ states (including $\Sigma_c^{(*)}\bar{D}^{(*)}$ and $\Lambda_c D^{(*)}$ systems) in the molecular model. For the convenience of calculation, Table VI lists the possible spin wave functions of the S -wave $\Sigma_c^{(*)}\bar{D}^{(*)}$ and $\Lambda_c D^{(*)}$ systems. We take $\mu_{\Sigma_c \bar{D}^* |^2 S_{1/2} \rangle \rightarrow \Sigma_c \bar{D} |^2 S_{1/2} \rangle}$ as an example to illustrate the procedure of getting the magnetic moments between the S -wave $\Sigma_c^{(*)}\bar{D}^{(*)}$ -type doubly charmed molecular pentaquark states. According to Table I and Table VI, the flavor-spin wave functions of the $\Sigma_c \bar{D}^* |^2 S_{1/2} \rangle$ and $\Sigma_c \bar{D} |^2 S_{1/2} \rangle$ states with $(I, I_3) = (\frac{1}{2}, -\frac{1}{2})$ can be con-

structed as

$$\begin{aligned} \psi_{\Sigma_c \bar{D}^* |^2 S_{1/2} \rangle} &= \left[\sqrt{\frac{1}{3}} |\Sigma_c^+ D^{*-} \rangle - \sqrt{\frac{2}{3}} |\Sigma_c^0 \bar{D}^{*0} \rangle \right] \otimes \\ &\quad \left[\sqrt{\frac{1}{3}} \left| \frac{1}{2}, \frac{1}{2} \right\rangle |1, 0\rangle - \sqrt{\frac{2}{3}} \left| \frac{1}{2}, -\frac{1}{2} \right\rangle |1, 1\rangle \right], \\ \psi_{\Sigma_c \bar{D} |^2 S_{1/2} \rangle} &= \left[\sqrt{\frac{1}{3}} |\Sigma_c^+ D^- \rangle - \sqrt{\frac{2}{3}} |\Sigma_c^0 \bar{D}^0 \rangle \right] \otimes \\ &\quad \left| \frac{1}{2}, \frac{1}{2} \right\rangle |0, 0\rangle. \end{aligned} \quad (15)$$

The transition magnetic moment of the $\Sigma_c \bar{D}^* |^2 S_{1/2} \rangle \rightarrow \Sigma_c \bar{D} |^2 S_{1/2} \rangle_\gamma$ process is

$$\begin{aligned} \mu_{\Sigma_c \bar{D}^* |^2 S_{1/2} \rangle \rightarrow \Sigma_c \bar{D} |^2 S_{1/2} \rangle} &= \langle \psi_{\Sigma_c \bar{D} |^2 S_{1/2} \rangle} | \hat{\mu}_z | \psi_{\Sigma_c \bar{D}^* |^2 S_{1/2} \rangle} \rangle \\ &= \frac{\sqrt{3}}{9} \mu_{D^{*-} \rightarrow D^-} + \frac{2\sqrt{3}}{9} \mu_{\bar{D}^{*0} \rightarrow \bar{D}^0}. \end{aligned} \quad (16)$$

Similarly, we obtain the transition magnetic moments of the S -wave hidden-charm pentaquark states in the molecular model. The transition magnetic moments between the S -wave $\Sigma_c^{(*)}\bar{D}^{(*)}$ -type hidden-charm molecular pentaquarks with isospin $(I, I_3) = (\frac{1}{2}, -\frac{1}{2})$ are collected in Table VII. The transition magnetic moments between the S -wave $\Sigma_c^{(*)}\bar{D}^{(*)}$ -type hidden-charm molecular pentaquarks with isospin $(I, I_3) = (\frac{3}{2}, -\frac{1}{2})$ are collected in Table IX. The transition magnetic moments between the S -wave $\Lambda_c D^{(*)}$ -type hidden-charm molecular pentaquarks with isospin $(I, I_3) = (\frac{1}{2}, -\frac{1}{2})$ are collected in Table VIII. In the S -wave $\Sigma_c^{(*)}\bar{D}^{(*)}$ -type hidden-charm molecular pentaquarks, the transition magnetic moments of the $\Sigma_c^* \bar{D}^* |^2 S_{1/2} \rangle \rightarrow \Sigma_c \bar{D}^* |^2 S_{1/2} \rangle_\gamma$ and $\Sigma_c^* \bar{D}^* |^6 S_{5/2} \rangle \rightarrow \Sigma_c^* \bar{D}^* |^2 S_{1/2} \rangle_\gamma$ processes are zero.

The transition magnetic moments we obtain are only prediction results at the quark level. Whether they correspond to the hadron-level results needs further studies. In Ref. [63], it is found that a scale factor probably exists for the coupling constants between the quark-level calculation and the hadron-level measurement by noticing that spin-different baryons are involved. Since the transition magnetic moment is also a coupling parameter in the hadron-level Lagrangian, we speculate that similar factors are also needed in linking the experiment data and our results if the proposal is correct. For the transition magnetic moment $|\frac{3}{2}\rangle \rightarrow |\frac{1}{2}\rangle\gamma$, the factor is $\sqrt{\frac{3}{2}}$, but such factors are currently unknown for other cases

TABLE VI: The spin wave functions of the S -wave $\Sigma_c^{(*)}\bar{D}^{(*)}$ and $\Lambda_c D^{(*)}$ systems. Where S and S_z are the spin and its third component of the investigated system, respectively.

Systems	$ S, S_z\rangle$	Spin wave functions
$\Sigma_c\bar{D}(\Lambda_c D)$	$ \frac{1}{2}, \frac{1}{2}\rangle$	$ \frac{1}{2}, \frac{1}{2}\rangle 0, 0\rangle$
$\Sigma_c^*\bar{D}$	$ \frac{3}{2}, \frac{3}{2}\rangle$	$ \frac{3}{2}, \frac{3}{2}\rangle 0, 0\rangle$
	$ \frac{3}{2}, \frac{1}{2}\rangle$	$ \frac{3}{2}, \frac{1}{2}\rangle 0, 0\rangle$
$\Sigma_c\bar{D}^*(\Lambda_c D^*)$	$ \frac{1}{2}, \frac{1}{2}\rangle$	$\sqrt{\frac{1}{3}} \frac{1}{2}, \frac{1}{2}\rangle 1, 0\rangle - \sqrt{\frac{2}{3}} \frac{1}{2}, -\frac{1}{2}\rangle 1, 1\rangle$
	$ \frac{3}{2}, \frac{3}{2}\rangle$	$ \frac{1}{2}, \frac{1}{2}\rangle 1, 1\rangle$
	$ \frac{3}{2}, \frac{1}{2}\rangle$	$\sqrt{\frac{2}{3}} \frac{1}{2}, \frac{1}{2}\rangle 1, 0\rangle + \sqrt{\frac{1}{3}} \frac{1}{2}, -\frac{1}{2}\rangle 1, 1\rangle$
$\Sigma_c^*\bar{D}^*$	$ \frac{1}{2}, \frac{1}{2}\rangle$	$\sqrt{\frac{1}{2}} \frac{3}{2}, \frac{3}{2}\rangle 1, -1\rangle - \sqrt{\frac{1}{3}} \frac{3}{2}, \frac{1}{2}\rangle 1, 0\rangle + \sqrt{\frac{1}{6}} \frac{3}{2}, -\frac{1}{2}\rangle 1, 1\rangle$
	$ \frac{3}{2}, \frac{3}{2}\rangle$	$\sqrt{\frac{3}{5}} \frac{3}{2}, \frac{3}{2}\rangle 1, 0\rangle - \sqrt{\frac{2}{5}} \frac{3}{2}, \frac{1}{2}\rangle 1, 1\rangle$
	$ \frac{3}{2}, \frac{1}{2}\rangle$	$\sqrt{\frac{2}{5}} \frac{3}{2}, \frac{3}{2}\rangle 1, -1\rangle + \sqrt{\frac{1}{15}} \frac{3}{2}, \frac{1}{2}\rangle 1, 0\rangle - \sqrt{\frac{8}{15}} \frac{3}{2}, -\frac{1}{2}\rangle 1, 1\rangle$
	$ \frac{5}{2}, \frac{5}{2}\rangle$	$ \frac{3}{2}, \frac{3}{2}\rangle 1, 1\rangle$
	$ \frac{5}{2}, \frac{3}{2}\rangle$	$\sqrt{\frac{2}{5}} \frac{3}{2}, \frac{3}{2}\rangle 1, 0\rangle + \sqrt{\frac{3}{5}} \frac{3}{2}, \frac{1}{2}\rangle 1, 1\rangle$
	$ \frac{5}{2}, \frac{1}{2}\rangle$	$\sqrt{\frac{1}{10}} \frac{3}{2}, \frac{3}{2}\rangle 1, -1\rangle + \sqrt{\frac{3}{5}} \frac{3}{2}, \frac{1}{2}\rangle 1, 0\rangle + \sqrt{\frac{3}{10}} \frac{3}{2}, -\frac{1}{2}\rangle 1, 1\rangle$

IV. MAGNETIC MOMENTS OF THE $P_\psi^{N^0}$ STATES AND $P_\psi^{\Delta^0}$ STATES IN THE DIQUARK-DIQUARK-ANTIQUARK MODEL

The magnetic moment formula of hidden-charm pentaquark states $(cq_3)(q_1q_2)\bar{c}$ in the diquark-diquark-antiquark model is

$$\begin{aligned}
\mu &= \langle \psi | g_{cq_3}\mu_{cq_3}\vec{S}_{cq_3} + g_{q_1q_2}\mu_{q_1q_2}\vec{S}_{q_1q_2} + g_{\bar{c}}\mu_{\bar{c}}\vec{S}_{\bar{c}} + \mu_l\vec{l} | \psi \rangle \\
&= \sum_{S_z, l_z} \langle SS_z, ll_z | JJ_z \rangle^2 \left\{ \mu_l l_z + \sum_{S'_1} \langle S_1 S'_1, S_{\bar{c}}(S_z - S'_1) | SS_z \rangle^2 \left[2(S_z - S'_1)\mu_{\bar{c}} + \sum_{S'_{cq_3}} \langle S_{cq_3} S'_{cq_3}, S_{q_1q_2}(S'_1 - S'_{cq_3}) | S_1 S'_1 \rangle^2 (S'_{cq_3}(\mu_{\bar{c}} + \mu_{q_3}) + (S'_1 - S'_{cq_3})(\mu_{q_1} + \mu_{q_2})) \right] \right\}, \quad (17)
\end{aligned}$$

where the subscripts cq_3 and q_1q_2 represent the diquark (cq_3) and (q_1q_2), respectively. S_{cq_3} and $S_{q_1q_2}$ couple into the spin S_1 , and the spin coupling of S_1 and $S_{\bar{c}}$ forms the total spin S of the pentaquark state. l is the orbital excitation. S'_1 , S_z and S'_{cq_3} are spin third component of (cq_3)(q_1q_2), pentaquark state and diquark (cq_3). ψ is the flavor wave function in diquark-diquark-antiquark model in Table I.

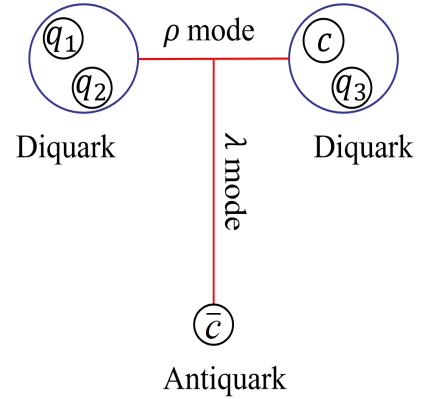


FIG. 1: Two excitation modes of P -wave in diquark-diquark-antiquark model.

In the diquark-diquark-antiquark model, P -wave orbital excitation includes ρ mode and λ mode. The P -wave orbital excitation of the ρ mode lies between diquark (cq_3) and diquark (q_1q_2). The P -wave orbital excitation of the λ mode lies between the \bar{c} and the center of mass system of diquark (cq_3) and diquark (q_1q_2). We show these two excitation modes in the Fig. 1. The

TABLE VII: Transition magnetic moments between the S -wave $\Sigma_c^{(*)}\bar{D}^{(*)}$ -type hidden-charm molecular pentaquarks $P_\psi^{N^0}$ with 8_{1f} flavor representation. The unit is the nuclear magnetic moment μ_N .

Decay modes	Expressions	Results
$\Sigma_c\bar{D}^* \frac{1}{2}^- \rangle \rightarrow \Sigma_c\bar{D} \frac{1}{2}^- \rangle\gamma$	$\frac{\sqrt{3}}{9}(\mu_{D^{*-}\rightarrow D^-} + 2\mu_{\bar{D}^{*0}\rightarrow \bar{D}^0})$	-0.780
$\Sigma_c\bar{D}^* \frac{3}{2}^- \rangle \rightarrow \Sigma_c\bar{D} \frac{1}{2}^- \rangle\gamma$	$\frac{\sqrt{6}}{9}(\mu_{D^{*-}\rightarrow D^-} + 2\mu_{\bar{D}^{*0}\rightarrow \bar{D}^0})$	-1.103
$\Sigma_c\bar{D}^* \frac{3}{2}^- \rangle \rightarrow \Sigma_c\bar{D}^* \frac{1}{2}^- \rangle\gamma$	$\frac{\sqrt{2}}{9}(2\mu_{\Sigma_c^+} + 4\mu_{\Sigma_c^0}) - \frac{\sqrt{2}}{9}(\mu_{D^{*-}} + 2\mu_{\bar{D}^{*0}})$	-0.979
$\Sigma_c^*\bar{D}^* \frac{1}{2}^- \rangle \rightarrow \Sigma_c\bar{D}^* \frac{3}{2}^- \rangle\gamma$	$-\frac{\sqrt{2}}{6}(\mu_{\Sigma_c^{*+}\rightarrow \Sigma_c^+} + 2\mu_{\Sigma_c^{*0}\rightarrow \Sigma_c^0})$	0.585
$\Sigma_c^*\bar{D} \frac{3}{2}^- \rangle \rightarrow \Sigma_c\bar{D} \frac{1}{2}^- \rangle\gamma$	$\frac{1}{3}(\mu_{\Sigma_c^{*+}\rightarrow \Sigma_c^+} + 2\mu_{\Sigma_c^{*0}\rightarrow \Sigma_c^0})$	-0.827
$\Sigma_c^*\bar{D}^* \frac{1}{2}^- \rangle \rightarrow \Sigma_c^*\bar{D} \frac{3}{2}^- \rangle\gamma$	$-\frac{\sqrt{3}}{9}(\mu_{D^{*-}\rightarrow D^-} + 2\mu_{\bar{D}^{*0}\rightarrow \bar{D}^0})$	0.780
$\Sigma_c^*\bar{D}^* \frac{3}{2}^- \rangle \rightarrow \Sigma_c\bar{D}^* \frac{1}{2}^- \rangle\gamma$	$-\frac{\sqrt{5}}{15}(\mu_{\Sigma_c^{*+}\rightarrow \Sigma_c^+} + 2\mu_{\Sigma_c^{*0}\rightarrow \Sigma_c^0})$	0.370
$\Sigma_c^*\bar{D}^* \frac{3}{2}^- \rangle \rightarrow \Sigma_c^*\bar{D}^* \frac{1}{2}^- \rangle\gamma$	$\frac{\sqrt{5}}{75}(2\mu_{\Sigma_c^{*+}} + 4\mu_{\Sigma_c^{*0}}) - \frac{\sqrt{5}}{75}(3\mu_{D^{*-}} + 6\mu_{\bar{D}^{*0}})$	-0.676
$\Sigma_c^*\bar{D}^* \frac{3}{2}^- \rangle \rightarrow \Sigma_c\bar{D}^* \frac{3}{2}^- \rangle\gamma$	$-\frac{\sqrt{10}}{15}(\mu_{\Sigma_c^{*+}\rightarrow \Sigma_c^+} + 2\mu_{\Sigma_c^{*0}\rightarrow \Sigma_c^0})$	0.523
$\Sigma_c^*\bar{D}^* \frac{3}{2}^- \rangle \rightarrow \Sigma_c^*\bar{D} \frac{3}{2}^- \rangle\gamma$	$\frac{\sqrt{15}}{15}(\mu_{D^{*-}\rightarrow D^-} + 2\mu_{\bar{D}^{*0}\rightarrow \bar{D}^0})$	-1.046
$\Sigma_c^*\bar{D}^* \frac{5}{2}^- \rangle \rightarrow \Sigma_c\bar{D}^* \frac{1}{2}^- \rangle\gamma$	$\frac{2\sqrt{5}}{15}(\mu_{\Sigma_c^{*+}\rightarrow \Sigma_c^+} + 2\mu_{\Sigma_c^{*0}\rightarrow \Sigma_c^0})$	-0.740
$\Sigma_c^*\bar{D}^* \frac{5}{2}^- \rangle \rightarrow \Sigma_c^*\bar{D} \frac{3}{2}^- \rangle\gamma$	$\frac{\sqrt{10}}{15}(\mu_{D^{*-}\rightarrow D^-} + 2\mu_{\bar{D}^{*0}\rightarrow \bar{D}^0})$	-0.854
$\Sigma_c^*\bar{D}^* \frac{5}{2}^- \rangle \rightarrow \Sigma_c\bar{D}^* \frac{3}{2}^- \rangle\gamma$	$\frac{\sqrt{15}}{15}(\mu_{\Sigma_c^{*+}\rightarrow \Sigma_c^+} + 2\mu_{\Sigma_c^{*0}\rightarrow \Sigma_c^0})$	-0.641
$\Sigma_c^*\bar{D}^* \frac{5}{2}^- \rangle \rightarrow \Sigma_c^*\bar{D}^* \frac{3}{2}^- \rangle\gamma$	$\frac{\sqrt{6}}{45}(2\mu_{\Sigma_c^{*+}} + 4\mu_{\Sigma_c^{*0}}) - \frac{\sqrt{6}}{45}(3\mu_{D^{*-}} + 6\mu_{\bar{D}^{*0}})$	-0.444

TABLE VIII: Transition magnetic moments between the S -wave $\Lambda_c D^{(*)}$ -type hidden-charm molecular pentaquarks $P_\psi^{N^0}$ with 8_{2f} flavor representation. The unit is the nuclear magnetic moment μ_N .

Decay modes	Expressions	Results
$\Lambda_c D^* \frac{1}{2}^- \rangle \rightarrow \Lambda_c D \frac{1}{2}^- \rangle\gamma$	$\frac{\sqrt{3}}{3}\mu_{D^{*-}\rightarrow D^-}$	0.314
$\Lambda_c D^* \frac{3}{2}^- \rangle \rightarrow \Lambda_c D^* \frac{1}{2}^- \rangle\gamma$	$\frac{\sqrt{2}}{3}(2\mu_{\Lambda_c^+} - \mu_{D^{*-}})$	1.017
$\Lambda_c D^* \frac{3}{2}^- \rangle \rightarrow \Lambda_c D \frac{1}{2}^- \rangle\gamma$	$\frac{\sqrt{6}}{3}\mu_{D^{*-}\rightarrow D^-}$	0.444

orbital magnetic moment μ_l in ρ mode and λ mode is

$$\rho \text{ mode : } \quad \mu_l = \frac{m_{q_1 q_2} \mu_{cq_3} + m_{cq_3} \mu_{q_1 q_2}}{m_{cq_3} + m_{q_1 q_2}}, \quad (18)$$

$$\lambda \text{ mode : } \quad \mu_l = \frac{m_{\bar{c}} \mu_{(cq_3)(q_1 q_2)} + m_{(cq_3)(q_1 q_2)} \mu_{\bar{c}}}{m_{(cq_3)(q_1 q_2)} + m_{\bar{c}}}, \quad (19)$$

$$m_{(cq_3)(q_1 q_2)} = \frac{m_{q_1 q_2} m_{cq_3}}{m_{cq_3} + m_{q_1 q_2}}, \quad (20)$$

where m and μ represent the mass and magnetic moment

of clusters represented by their subscripts. For example, $m_{q_1 q_2}$ represents the mass of diquark $q_1 q_2$. The mass of diquarks in diquark-diquark-antiquark model are [64]:

$$\begin{aligned} m_{[q,q]} &= 0.710 \text{ GeV}, & m_{\{q,q\}} &= 0.909 \text{ GeV}, \\ m_{[c,q]} &= 1.937 \text{ GeV}, & m_{\{c,q\}} &= 2.036 \text{ GeV}. \end{aligned} \quad (21)$$

The magnetic moments of the S -wave $P_\psi^{N^0}$ states and $P_\psi^{\Delta^0}$ states are presented in Table X. The magnetic moments of the P -wave excitation $P_\psi^{N^0}$ states and $P_\psi^{\Delta^0}$ states in the λ mode and ρ mode are presented in Table XI -Table XIII.

V. MAGNETIC MOMENTS OF THE $P_\psi^{N^0}$ STATES AND $P_\psi^{\Delta^0}$ STATES IN THE DIQUARK-TRIQUARK MODEL

We calculated the magnetic moments in the diquark-triquark model with configurations $(cq_3)(\bar{c}q_1 q_2)$. Similar to the magnetic moments expression in the molecular

TABLE IX: Transition magnetic moments between the S -wave $\Sigma_c^{(*)}\bar{D}^{(*)}$ -type hidden-charm molecular pentaquarks $P_\psi^{\Delta^0}$ with 10_f flavor representation. The unit is the nuclear magnetic moment μ_N .

Decay modes	Expressions	Results
$\Sigma_c\bar{D}^* \frac{1}{2}^- \rangle \rightarrow \Sigma_c\bar{D} \frac{1}{2}^- \rangle\gamma$	$\frac{\sqrt{3}}{9}(2\mu_{D^{*-}\rightarrow D^-} + \mu_{\bar{D}^{*0}\rightarrow \bar{D}^0})$	-0.233
$\Sigma_c\bar{D}^* \frac{3}{2}^- \rangle \rightarrow \Sigma_c\bar{D} \frac{1}{2}^- \rangle\gamma$	$\frac{\sqrt{6}}{9}(2\mu_{D^{*-}\rightarrow D^-} + \mu_{\bar{D}^{*0}\rightarrow \bar{D}^0})$	-0.329
$\Sigma_c\bar{D}^* \frac{3}{2}^- \rangle \rightarrow \Sigma_c\bar{D}^* \frac{1}{2}^- \rangle\gamma$	$\frac{\sqrt{2}}{9}(4\mu_{\Sigma_c^+} + 2\mu_{\Sigma_c^0}) - \frac{\sqrt{2}}{9}(2\mu_{D^{*-}} + \mu_{\bar{D}^{*0}})$	0.063
$\Sigma_c^*\bar{D}^* \frac{1}{2}^- \rangle \rightarrow \Sigma_c\bar{D}^* \frac{3}{2}^- \rangle\gamma$	$-\frac{\sqrt{2}}{6}(2\mu_{\Sigma_c^+\rightarrow\Sigma_c^+} + \mu_{\Sigma_c^{*0}\rightarrow\Sigma_c^0})$	0.269
$\Sigma_c^*\bar{D} \frac{3}{2}^- \rangle \rightarrow \Sigma_c\bar{D} \frac{1}{2}^- \rangle\gamma$	$\frac{1}{3}(2\mu_{\Sigma_c^+\rightarrow\Sigma_c^+} + \mu_{\Sigma_c^{*0}\rightarrow\Sigma_c^0})$	-0.380
$\Sigma_c^*\bar{D}^* \frac{1}{2}^- \rangle \rightarrow \Sigma_c^*\bar{D} \frac{3}{2}^- \rangle\gamma$	$-\frac{\sqrt{3}}{9}(2\mu_{D^{*-}\rightarrow D^-} + \mu_{\bar{D}^{*0}\rightarrow \bar{D}^0})$	0.233
$\Sigma_c^*\bar{D}^* \frac{3}{2}^- \rangle \rightarrow \Sigma_c\bar{D}^* \frac{1}{2}^- \rangle\gamma$	$-\frac{\sqrt{5}}{15}(\mu_{\Sigma_c^+\rightarrow\Sigma_c^+} + \mu_{\Sigma_c^{*0}\rightarrow\Sigma_c^0})$	0.170
$\Sigma_c^*\bar{D}^* \frac{3}{2}^- \rangle \rightarrow \Sigma_c^*\bar{D}^* \frac{1}{2}^- \rangle\gamma$	$\frac{\sqrt{5}}{75}(4\mu_{\Sigma_c^+} + 2\mu_{\Sigma_c^0}) - \frac{\sqrt{5}}{75}(6\mu_{D^{*-}} - 3\mu_{\bar{D}^{*0}})$	0.501
$\Sigma_c^*\bar{D}^* \frac{3}{2}^- \rangle \rightarrow \Sigma_c\bar{D}^* \frac{3}{2}^- \rangle\gamma$	$-\frac{\sqrt{10}}{15}(2\mu_{\Sigma_c^+\rightarrow\Sigma_c^+} + \mu_{\Sigma_c^{*0}\rightarrow\Sigma_c^0})$	0.241
$\Sigma_c^*\bar{D}^* \frac{3}{2}^- \rangle \rightarrow \Sigma_c^*\bar{D} \frac{3}{2}^- \rangle\gamma$	$\frac{\sqrt{15}}{15}(2\mu_{D^{*-}\rightarrow D^-} + \mu_{\bar{D}^{*0}\rightarrow \bar{D}^0})$	-0.313
$\Sigma_c^*\bar{D}^* \frac{5}{2}^- \rangle \rightarrow \Sigma_c\bar{D}^* \frac{1}{2}^- \rangle\gamma$	$\frac{2\sqrt{5}}{15}(2\mu_{\Sigma_c^+\rightarrow\Sigma_c^+} + \mu_{\Sigma_c^{*0}\rightarrow\Sigma_c^0})$	-0.340
$\Sigma_c^*\bar{D}^* \frac{5}{2}^- \rangle \rightarrow \Sigma_c^*\bar{D} \frac{3}{2}^- \rangle\gamma$	$\frac{\sqrt{10}}{15}(2\mu_{D^{*-}\rightarrow D^-} + \mu_{\bar{D}^{*0}\rightarrow \bar{D}^0})$	-0.255
$\Sigma_c^*\bar{D}^* \frac{5}{2}^- \rangle \rightarrow \Sigma_c\bar{D}^* \frac{3}{2}^- \rangle\gamma$	$\frac{\sqrt{15}}{15}(2\mu_{\Sigma_c^+\rightarrow\Sigma_c^+} + \mu_{\Sigma_c^{*0}\rightarrow\Sigma_c^0})$	-0.295
$\Sigma_c^*\bar{D}^* \frac{5}{2}^- \rangle \rightarrow \Sigma_c^*\bar{D}^* \frac{3}{2}^- \rangle\gamma$	$\frac{\sqrt{6}}{45}(4\mu_{\Sigma_c^+} + 2\mu_{\Sigma_c^0}) - \frac{\sqrt{6}}{45}(6\mu_{D^{*-}} + 3\mu_{\bar{D}^{*0}})$	0.329

model, the magnetic moments in diquark-triquark model is

$$\begin{aligned}
\mu &= \langle \psi | g_{cq_3}\mu_{cq_3}\vec{S}_{cq_3} + g_{\bar{c}q_1q_2}\mu_{\bar{c}q_1q_2}\vec{S}_{\bar{c}q_1q_2} + \mu_l\vec{l} | \psi \rangle \\
&= \sum_{l_z, S_z} \langle ll_z, SS_z | JJ_z \rangle^2 \left\{ \sum_{S'_{\bar{c}q_1q_2}} \langle S_{\bar{c}q_1q_2} S'_{\bar{c}q_1q_2}, S_{cq_3} (S_z \right. \\
&\quad \left. - S'_{\bar{c}q_1q_2}) | SS_z \rangle^2 [(S_z - S'_{\bar{c}q_1q_2})(\mu_c + \mu_{q_3}) \right. \\
&\quad \left. + \sum_{S'_{\bar{c}}, S'_{q_1q_2}} \langle S_{\bar{c}} S'_{\bar{c}}, S_{q_1q_2} S'_{q_1q_2} | S_{\bar{c}q_1q_2} S'_{\bar{c}q_1q_2} \rangle^2 (g_{\bar{c}}\mu_{\bar{c}} S'_{\bar{c}} \right. \\
&\quad \left. + S'_{q_1q_2}(\mu_{q_1} + \mu_{q_2})) \right] + \mu_l l_z \left. \right\}, \quad (22)
\end{aligned}$$

where S_{cq_3} and $S_{\bar{c}q_1q_2}$ represent the spin of the diquark (cq_3) and the triquark ($\bar{c}q_1q_2$), respectively. $S_{q_1q_2}$ represent the spin of the diquark (q_1q_2) inside the triquark ($\bar{c}q_1q_2$). $S'_{\bar{c}q_1q_2}$, S_z and $S'_{q_1q_2}$ are spin third component of triquark ($\bar{c}q_1q_2$), pentaquark state and diquark (q_1q_2). $S_{\bar{c}}$ and $S'_{\bar{c}}$ are spin and third component of antiquark \bar{c} . ψ represents the flavor wave function in diquark-triquark model in Table I, The orbital magnetic moment

in diquark-triquark model is

$$\mu_l = \frac{m_{cq_3}\mu_{\bar{c}q_1q_2} + m_{\bar{c}q_1q_2}\mu_{cq_3}}{m_{\bar{c}q_1q_2} + m_{cq_3}}, \quad (23)$$

where m and μ are the mass and magnetic moment of the cluster represented by their subscripts. The mass of the triquarks is roughly equal to the sum of the mass of the corresponding diquarks and antiquarks [51]. Here, we use the values of the diquark masses from Eq. (21). The magnetic moments and corresponding expressions in the diquark-triquark mode are presented in Table XIV and Table XV.

VI. NUMERICAL ANALYSIS

The analysis of magnetic moments and transition magnetic moments of pentaquark states is an effective method to explore their inner structures. This is an important work for the later discovery of the $P_\psi^{N^0}$ states and $P_\psi^{\Delta^0}$ states, and opens up another way for us to ex-

TABLE X: The magnetic moments of the S -wave $P_\psi^{N^0}$ states in the diquark-diquark-antiquark model with the 8_{2f} and 8_{1f} flavor representation, and the magnetic moments of the S -wave $P_\psi^{\Delta^0}$ states in the diquark-diquark-antiquark model with the 10_f flavor representation. The $J_1^{P_1} \otimes J_2^{P_2} \otimes J_3^{P_3} \otimes J_4^{P_4}$ are corresponding to the angular momentum and parity of (cq_1) , (q_2q_3) , \bar{c} and orbital, respectively. The unit is the nuclear magnetic moment μ_N .

$(cd)[ud]\bar{c}$				
J^P	$^{2s+1}L_J$	$J_1^{P_1} \otimes J_2^{P_2} \otimes J_3^{P_3} \otimes J_4^{P_4}$	Expressions	Results
$\frac{1}{2}^-$	$^2S_{\frac{1}{2}}$	$0^+ \otimes 0^+ \otimes \frac{1}{2}^- \otimes 0^+$	$-\mu_c$	-0.403
		$1^+ \otimes 0^+ \otimes \frac{1}{2}^- \otimes 0^+$	$\frac{1}{3}(3\mu_c + 2\mu_d)$	-0.228
$\frac{3}{2}^-$	$^4S_{\frac{3}{2}}$	$1^+ \otimes 0^+ \otimes \frac{1}{2}^- \otimes 0^+$	μ_d	-0.947
$\sqrt{\frac{1}{3}}(cd)\{ud\}\bar{c} - \sqrt{\frac{2}{3}}(cu)\{dd\}\bar{c}$				
J^P	$^{2s+1}L_J$	$J_1^{P_1} \otimes J_2^{P_2} \otimes J_3^{P_3} \otimes J_4^{P_4}$	Expressions	Results
$\frac{1}{2}^-$	$^2S_{\frac{1}{2}}$	$0^+ \otimes 1^+ \otimes \frac{1}{2}^- \otimes 0^+$	$\frac{1}{3}(2\mu_u + 10\mu_d + 3\mu_c)$	-1.492
		$(1^+ \otimes 1^+)_0 \otimes \frac{1}{2}^- \otimes 0^+$	$-\mu_c$	-0.403
		$(1^+ \otimes 1^+)_1 \otimes \frac{1}{2}^- \otimes 0^+$	$\frac{1}{9}(3\mu_u + 6\mu_d + 6\mu_c)$	0.269
$\frac{3}{2}^-$	$^4S_{\frac{3}{2}}$	$(0^+ \otimes 1^+) \otimes \frac{1}{2}^- \otimes 0^+$	$\frac{1}{3}(\mu_u + 5\mu_d - 3\mu_c)$	-1.351
		$(1^+ \otimes 1^+)_1 \otimes \frac{1}{2}^- \otimes 0^+$	$\frac{1}{2}(\mu_u + 2\mu_d - \mu_c)$	-0.202
		$(1^+ \otimes 1^+)_2 \otimes \frac{1}{2}^- \otimes 0^+$	$\frac{3}{10}(3\mu_u + 6\mu_d + 5\mu_c)$	0.605
$\frac{5}{2}^-$	$^6S_{\frac{5}{2}}$	$1^+ \otimes 1^+ \otimes \frac{1}{2}^- \otimes 0^+$	$\mu_u + 2\mu_d$	0
$\sqrt{\frac{2}{3}}(cd)\{ud\}\bar{c} + \sqrt{\frac{1}{3}}(cu)\{dd\}\bar{c}$				
J^P	$^{2s+1}L_J$	$J_1^{P_1} \otimes J_2^{P_2} \otimes J_3^{P_3} \otimes J_4^{P_4}$	Expressions	Results
$\frac{1}{2}^-$	$^2S_{\frac{1}{2}}$	$0^+ \otimes 1^+ \otimes \frac{1}{2}^- \otimes 0^+$	$\frac{1}{3}(4\mu_u + 8\mu_d + 3\mu_c)$	0.403
		$(1^+ \otimes 1^+)_0 \otimes \frac{1}{2}^- \otimes 0^+$	$-\mu_c$	-0.403
		$(1^+ \otimes 1^+)_1 \otimes \frac{1}{2}^- \otimes 0^+$	$\frac{1}{9}(3\mu_u + 6\mu_d + 6\mu_c)$	0.269
$\frac{3}{2}^-$	$^4S_{\frac{3}{2}}$	$(0^+ \otimes 1^+) \otimes \frac{1}{2}^- \otimes 0^+$	$\frac{1}{3}(2\mu_u + 4\mu_d - 3\mu_c)$	-0.403
		$(1^+ \otimes 1^+)_1 \otimes \frac{1}{2}^- \otimes 0^+$	$\frac{1}{2}(\mu_u + 2\mu_d - \mu_c)$	-0.202
		$(1^+ \otimes 1^+)_2 \otimes \frac{1}{2}^- \otimes 0^+$	$\frac{3}{10}(3\mu_u + 6\mu_d + 5\mu_c)$	0.605
$\frac{5}{2}^-$	$^6S_{\frac{5}{2}}$	$1^+ \otimes 1^+ \otimes \frac{1}{2}^- \otimes 0^+$	$\mu_u + 2\mu_d$	0

plore the exotic hadrons. In this work, we systematically calculate the magnetic moments of $P_\psi^{N^0}$ states and $P_\psi^{\Delta^0}$ states in diquark-diquark-antiquark model and diquark-triquark model, and also calculate the magnetic moments and transition magnetic moments of $P_\psi^{N^0}$ states and $P_\psi^{\Delta^0}$ states in molecular model. In this section, we will analyze the results of magnetic moments and transition magnetic moments respectively.

A. Magnetic moments of the $P_\psi^{N^0}$ and $P_\psi^{\Delta^0}$ states in molecular model, diquark-diquark-antiquark model and diquark-triquark model

We calculate the magnetic moments of the $P_\psi^{N^0}$ states and $P_\psi^{\Delta^0}$ states in three models. On the basis of the magnetic moment results obtained in this work, we summarized the following key points.

- In the diquark-diquark-antiquark model, the ρ mode and the λ mode in the P -wave excitation will lead to obvious difference in magnetic moment. The magnetic moments in Table XI -Table XIII indicate that the magnetic moments of the λ excitation state are usually larger than

TABLE XI: The excited state magnetic moments of the $P_\psi^{N^0}$ states in the diquark-diquark-antiquark model with the 8_{2f} flavor representation. In the λ mode P -wave excitation, $\mu_{l(S_{cd} \otimes S_{ud}/S_{\bar{c}})}$ represents the orbital magnetic moment between \bar{c} and center of mass system of diquark (cd) and diquark (ud), S_{cd} , S_{ud} and $S_{\bar{c}}$ represent the spins of diquark (cd), diquark (ud) and \bar{c} , respectively. In the ρ mode P -wave excitation, $\mu_{l(S_{cd}/S_{ud})}$ represents the orbital magnetic moment between diquark (cd) and diquark (ud), S_{cd} and S_{ud} represent the spins of diquark (cd) and diquark (ud), respectively. The $J_1^{P_1} \otimes J_2^{P_2} \otimes J_3^{P_3} \otimes J_4^{P_4}$ are corresponding to the angular momentum and parity of (cq_1), (q_2q_3), \bar{c} and orbital, respectively. The unit is the nuclear magnetic moment μ_N .

$(cd)[ud]\bar{c}$				
J^P	$^{2s+1}L_J$	$J_1^{P_1} \otimes J_2^{P_2} \otimes J_3^{P_3} \otimes J_4^{P_4}$	Expressions	Results
$\frac{1}{2}^+$	$^2P_{\frac{1}{2}}$	$0^+ \otimes 0^+ \otimes \frac{1}{2}^- \otimes 1^-$	$\frac{1}{3} (\mu_c + 2\mu_{l(0 \otimes 0/\frac{1}{2})})$	$0.669_{(\lambda)}$
		$\frac{1}{3} (\mu_c + 2\mu_{l(0/0)})$	$0.378_{(\rho)}$	
	$^4P_{\frac{1}{2}}$	$(1^+ \otimes 0^+ \otimes \frac{1}{2}^-)_{\frac{1}{2}} \otimes 1^-$	$\frac{1}{9} (-3\mu_c - 2\mu_d + 6\mu_{l(1 \otimes 0/\frac{1}{2})})$	$0.599_{(\lambda)}$
		$\frac{1}{9} (-3\mu_c - 2\mu_d + 6\mu_{l(1/0)})$	$0.320_{(\rho)}$	
$\frac{3}{2}^+$	$^2P_{\frac{3}{2}}$	$0^+ \otimes 0^+ \otimes \frac{1}{2}^- \otimes 1^-$	$-\mu_c + \mu_{l(0 \otimes 0/\frac{1}{2})}$	$0.399_{(\lambda)}$
		$-\mu_c + \mu_{l(0/0)}$	$-0.038_{(\rho)}$	
	$^4P_{\frac{3}{2}}$	$(1^+ \otimes 0^+ \otimes \frac{1}{2}^-)_{\frac{1}{2}} \otimes 1^-$	$\frac{1}{3} (3\mu_c + 2\mu_d + 3\mu_{l(1 \otimes 0/\frac{1}{2})})$	$0.556_{(\lambda)}$
		$\frac{1}{3} (3\mu_c + 2\mu_d + 3\mu_{l(1/0)})$	$0.138_{(\rho)}$	
$^4P_{\frac{3}{2}}$	$(1^+ \otimes 0^+ \otimes \frac{1}{2}^-)_{\frac{3}{2}} \otimes 1^-$	$\frac{1}{15} (11\mu_d + 6\mu_{l(1 \otimes 0/\frac{1}{2})})$	$-0.381_{(\lambda)}$	
		$\frac{1}{15} (11\mu_d + 6\mu_{l(1/0)})$	$-0.548_{(\rho)}$	
$\frac{5}{2}^+$	$^4P_{\frac{5}{2}}$	$1^+ \otimes 0^+ \otimes \frac{1}{2}^- \otimes 1^-$	$\mu_d + \mu_{l(1 \otimes 0/\frac{1}{2})}$	$-0.163_{(\lambda)}$
			$\mu_d + \mu_{l(1/0)}$	$-0.581_{(\rho)}$

the magnetic moments of the ρ excitation state. This is caused by the orbital magnetic moment $\mu_{l\lambda} > \mu_{l\rho}$. In order to facilitate analysis and comparison, we have shown the excited state magnetic moment results of these two excitation modes in Fig. 2, Fig. 3 and Fig. 4.

In Fig. 2 and Fig. 3, we find that in the interval of quantum number $J^P = \frac{1}{2}^+$ and $J^P = \frac{3}{2}^+$, there are a few magnetic moments of the ρ excitation state are larger than magnetic moments of the λ excitation state. Their spin configurations are

$$\begin{aligned}
J^P = \frac{1}{2}^+ : & \quad (0^+ \otimes 1^+ \otimes \frac{1}{2}^-)_{\frac{3}{2}} \otimes 1^-, \\
& \quad ((1^+ \otimes 1^+)_{1} \otimes \frac{1}{2}^-)_{\frac{3}{2}} \otimes 1^-, \\
& \quad ((1^+ \otimes 1^+)_{2} \otimes \frac{1}{2}^-)_{\frac{3}{2}} \otimes 1^-. \quad (24)
\end{aligned}$$

$$J^P = \frac{3}{2}^+ : \quad ((1^+ \otimes 1^+)_{2} \otimes \frac{1}{2}^-)_{\frac{5}{2}} \otimes 1^-. \quad (25)$$

In the interval of quantum number $J^P = \frac{5}{2}^+$ and $J^P = \frac{7}{2}^+$, the magnetic moments of the λ excitation state are

all larger than the magnetic moments of the ρ excitation state.

In Fig. 4, we find that except for the interval of quantum number $J^P = \frac{1}{2}^+$, there is a group of the magnetic moments of the ρ excitation state are larger than the magnetic moments of the λ excitation state, other the magnetic moments of the λ excitation state are larger than the magnetic moments of the ρ excitation state. Its spin configuration is

$$J^P = \frac{1}{2}^+ : \quad (1^+ \otimes 0^+ \otimes \frac{1}{2}^-)_{\frac{3}{2}} \otimes 1^-. \quad (26)$$

In other words, with the increase of the quantum number J^P , the phenomenon that the magnetic moments of the λ excitation state are larger than the magnetic moments of the ρ excitation state becomes more obvious.

• In Table X, the magnetic moment expressions of S -wave $P_\psi^{N^0}$ states with 8_{1f} flavor representation and S -wave $P_\psi^{\Delta^0}$ states with 10_f flavor representation are equal whose spin configurations satisfying $J_1^{P_1} \otimes J_2^{P_2} \otimes J_3^{P_3} \otimes$

TABLE XII: The excited state magnetic moments of the P_ψ^{N0} states in the diquark-diquark-antiquark model with the 8_{1f} flavor representation. In the λ mode P -wave excitation, $\mu_{l(S_{cd}\otimes S_{ud}/S_{\bar{c}})}$ represents the orbital magnetic moment between \bar{c} and center of mass system of diquark (cd) and diquark (ud), S_{cd} , S_{ud} and $S_{\bar{c}}$ represent the spins of diquark (cd), diquark (ud) and \bar{c} , respectively. $\mu_{l'(S_{cu}\otimes S_{dd}/S_{\bar{c}})}$ represents the orbital magnetic moment between \bar{c} and center of mass system of diquark (cu) and diquark (dd), and S_{cu} , S_{dd} and $S_{\bar{c}}$ represent the spins of diquark (cu), diquark (dd) and \bar{c} , respectively. In the ρ mode P -wave excitation, $\mu_{l(S_{cd}/S_{ud})}$ represents the orbital magnetic moment between diquark (cd) and diquark (ud), S_{cd} and S_{ud} represent the spins of diquark (cd) and diquark (ud), respectively. $\mu_{l'(S_{cu}/S_{dd})}$ represents the orbital magnetic moment between diquark (cu) and diquark (dd), S_{cu} and S_{dd} represent the spins of diquark (cu), diquark (dd), respectively. The $J_1^{P_1} \otimes J_2^{P_2} \otimes J_3^{P_3} \otimes J_4^{P_4}$ are corresponding to the angular momentum and parity of (cq_1), (q_2q_3), \bar{c} and orbital, respectively. The unit is the nuclear magnetic moment μ_N .

$\sqrt{\frac{1}{3}}(cd)\{ud\}\bar{c} - \sqrt{\frac{2}{3}}(cu)\{dd\}\bar{c}$					
J^P	$2s+1L_J$	$J_1^{P_1} \otimes J_2^{P_2} \otimes J_3^{P_3} \otimes J_4^{P_4}$	Expressions	Results	
$\frac{1}{2}^+$	${}^2P_{\frac{1}{2}}$	$(0^+ \otimes 1^+ \otimes \frac{1}{2}^-)_{\frac{1}{2}} \otimes 1^-$	$\frac{1}{27}(-2\mu_u - 10\mu_d - 3\mu_c + 6\mu_{l(0\otimes 1/\frac{1}{2})} + 12\mu_{l'(0\otimes 1/\frac{1}{2})})$ $\frac{1}{27}(-2\mu_u - 10\mu_d - 3\mu_c + 6\mu_{l(0/1)} + 12\mu_{l'(0/1)})$	$0.570_{(\lambda)}$ $0.112_{(\rho)}$	
		$((1^+ \otimes 1^+)_0 \otimes \frac{1}{2}^-)_{\frac{1}{2}} \otimes 1^-$	$\frac{1}{9}(3\mu_c + 2\mu_{l(1\otimes 1/\frac{1}{2})} + 4\mu_{l'(1\otimes 1/\frac{1}{2})})$ $\frac{1}{9}(3\mu_c + 2\mu_{l(1/1)} + 4\mu_{l'(1/1)})$	$0.529_{(\lambda)}$ $0.071_{(\rho)}$	
		$((1^+ \otimes 1^+)_1 \otimes \frac{1}{2}^-)_{\frac{1}{2}} \otimes 1^-$	$\frac{1}{27}(-3\mu_u - 6\mu_d - 6\mu_c + 6\mu_{l(1\otimes 1/\frac{1}{2})} + 12\mu_{l'(1\otimes 1/\frac{1}{2})})$ $\frac{1}{27}(-3\mu_u - 6\mu_d - 6\mu_c + 6\mu_{l(1/1)} + 12\mu_{l'(1/1)})$	$0.305_{(\lambda)}$ $-0.153_{(\rho)}$	
	${}^4P_{\frac{1}{2}}$	$(0^+ \otimes 1^+ \otimes \frac{1}{2}^-)_{\frac{3}{2}} \otimes 1^-$	$\frac{1}{27}(5\mu_u + 25\mu_d - 15\mu_c - 3\mu_{l(0\otimes 1/\frac{1}{2})} - 6\mu_{l'(0\otimes 1/\frac{1}{2})})$ $\frac{1}{27}(5\mu_u + 25\mu_d - 15\mu_c - 3\mu_{l(0/1)} - 6\mu_{l'(0/1)})$	$-0.953_{(\lambda)}$ $-0.724_{(\rho)}$	
		$((1^+ \otimes 1^+)_1 \otimes \frac{1}{2}^-)_{\frac{3}{2}} \otimes 1^-$	$\frac{1}{54}(15\mu_u + 30\mu_d - 15\mu_c - 6\mu_{l(1\otimes 1/\frac{1}{2})} - 12\mu_{l'(1\otimes 1/\frac{1}{2})})$ $\frac{1}{54}(15\mu_u + 30\mu_d - 15\mu_c - 6\mu_{l(1/1)} - 12\mu_{l'(1/1)})$	$-0.309_{(\lambda)}$ $-0.080_{(\rho)}$	
		$((1^+ \otimes 1^+)_2 \otimes \frac{1}{2}^-)_{\frac{3}{2}} \otimes 1^-$	$\frac{1}{18}(15\mu_u + 18\mu_d + 15\mu_c - 2\mu_{l(1\otimes 1/\frac{1}{2})} - 4\mu_{l'(1\otimes 1/\frac{1}{2})})$ $\frac{1}{18}(15\mu_u + 18\mu_d + 15\mu_c - 2\mu_{l(1/1)} - 4\mu_{l'(1/1)})$	$0.140_{(\lambda)}$ $0.224_{(\rho)}$	
	$\frac{3}{2}^+$	${}^2P_{\frac{3}{2}}$	$(0^+ \otimes 1^+ \otimes \frac{1}{2}^-)_{\frac{1}{2}} \otimes 1^-$	$\frac{1}{9}(2\mu_u + 10\mu_d + 3\mu_c + 3\mu_{l(0\otimes 1/\frac{1}{2})} + 6\mu_{l'(0\otimes 1/\frac{1}{2})})$ $\frac{1}{9}(2\mu_u + 10\mu_d + 3\mu_c + 3\mu_{l(0/1)} + 6\mu_{l'(0/1)})$	$0.110_{(\lambda)}$ $-0.577_{(\rho)}$
			$((1^+ \otimes 1^+)_0 \otimes \frac{1}{2}^-)_{\frac{1}{2}} \otimes 1^-$	$\frac{1}{3}(-3\mu_c + \mu_{l(1\otimes 1/\frac{1}{2})} + 2\mu_{l'(1\otimes 1/\frac{1}{2})})$ $\frac{1}{3}(-3\mu_c + \mu_{l(1/1)} + 2\mu_{l'(1/1)})$	$0.186_{(\lambda)}$ $-0.499_{(\rho)}$
			$((1^+ \otimes 1^+)_1 \otimes \frac{1}{2}^-)_{\frac{1}{2}} \otimes 1^-$	$\frac{1}{9}(3\mu_u + 6\mu_d + 6\mu_c + 3\mu_{l(1\otimes 1/\frac{1}{2})} + 6\mu_{l'(1\otimes 1/\frac{1}{2})})$ $\frac{1}{9}(3\mu_u + 6\mu_d + 6\mu_c + 3\mu_{l(1/1)} + 6\mu_{l'(1/1)})$	$0.858_{(\lambda)}$ $0.174_{(\rho)}$
${}^4P_{\frac{3}{2}}$		$(0^+ \otimes 1^+ \otimes \frac{1}{2}^-)_{\frac{3}{2}} \otimes 1^-$	$\frac{1}{45}(11\mu_u + 55\mu_d - 33\mu_c + 6\mu_{l(0\otimes 1/\frac{1}{2})} + 12\mu_{l'(0\otimes 1/\frac{1}{2})})$ $\frac{1}{45}(11\mu_u + 55\mu_d - 33\mu_c + 6\mu_{l(0/1)} + 12\mu_{l'(0/1)})$	$-0.748_{(\lambda)}$ $-1.022_{(\rho)}$	
		$((1^+ \otimes 1^+)_1 \otimes \frac{1}{2}^-)_{\frac{3}{2}} \otimes 1^-$	$\frac{1}{90}(33\mu_u + 66\mu_d - 33\mu_c + 12\mu_{l(1\otimes 1/\frac{1}{2})} + 24\mu_{l'(1\otimes 1/\frac{1}{2})})$ $\frac{1}{90}(33\mu_u + 66\mu_d - 33\mu_c + 12\mu_{l(1/1)} + 24\mu_{l'(1/1)})$	$0.088_{(\lambda)}$ $-0.186_{(\rho)}$	
		$((1^+ \otimes 1^+)_2 \otimes \frac{1}{2}^-)_{\frac{3}{2}} \otimes 1^-$	$\frac{1}{150}(99\mu_u + 198\mu_d + 165\mu_c + 20\mu_{l(1\otimes 1/\frac{1}{2})} + 40\mu_{l'(1\otimes 1/\frac{1}{2})})$ $\frac{1}{150}(99\mu_u + 198\mu_d + 165\mu_c + 20\mu_{l(1/1)} + 40\mu_{l'(1/1)})$	$0.679_{(\lambda)}$ $0.406_{(\rho)}$	
${}^6P_{\frac{3}{2}}$		$((1^+ \otimes 1^+)_2 \otimes \frac{1}{2}^-)_{\frac{5}{2}} \otimes 1^-$	$\frac{1}{25}(14\mu_u + 42\mu_d - 5\mu_{l(1\otimes 1/\frac{1}{2})} - 10\mu_{l'(1\otimes 1/\frac{1}{2})})$ $\frac{1}{25}(14\mu_u + 42\mu_d - 5\mu_{l(1/1)} - 10\mu_{l'(1/1)})$	$-0.353_{(\lambda)}$ $0.057_{(\rho)}$	
$\frac{5}{2}^+$		${}^4P_{\frac{5}{2}}$	$(0^+ \otimes 1^+ \otimes \frac{1}{2}^-) \otimes 1^-$	$\frac{1}{3}(\mu_u + 5\mu_d - 3\mu_c + \mu_{l(0\otimes 1/\frac{1}{2})} + 2\mu_{l'(0\otimes 1/\frac{1}{2})})$ $\frac{1}{3}(\mu_u + 5\mu_d - 3\mu_c + \mu_{l(0/1)} + 2\mu_{l'(0/1)})$	$-0.744_{(\lambda)}$ $-1.430_{(\rho)}$
			$((1^+ \otimes 1^+)_1 \otimes \frac{1}{2}^-)_{\frac{3}{2}} \otimes 1^-$	$\frac{1}{6}(3\mu_u + 6\mu_d - 3\mu_c + 2\mu_{l(1\otimes 1/\frac{1}{2})} + 4\mu_{l'(1\otimes 1/\frac{1}{2})})$ $\frac{1}{6}(3\mu_u + 6\mu_d - 3\mu_c + 2\mu_{l(1/1)} + 4\mu_{l'(1/1)})$	$0.387_{(\lambda)}$ $-0.297_{(\rho)}$
	$((1^+ \otimes 1^+)_2 \otimes \frac{1}{2}^-)_{\frac{3}{2}} \otimes 1^-$		$\frac{1}{30}(27\mu_u + 54\mu_d + 15\mu_c + 10\mu_{l(1\otimes 1/\frac{1}{2})} + 20\mu_{l'(1\otimes 1/\frac{1}{2})})$ $\frac{1}{30}(27\mu_u + 54\mu_d + 15\mu_c + 10\mu_{l(1/1)} + 20\mu_{l'(1/1)})$	$1.194_{(\lambda)}$ $0.509_{(\rho)}$	
	${}^6P_{\frac{5}{2}}$	$((1^+ \otimes 1^+)_2 \otimes \frac{1}{2}^-)_{\frac{5}{2}} \otimes 1^-$	$\frac{1}{105}(93\mu_u + 186\mu_d + 10\mu_{l(1\otimes 1/\frac{1}{2})} + 20\mu_{l'(1\otimes 1/\frac{1}{2})})$ $\frac{1}{105}(93\mu_u + 186\mu_d + 10\mu_{l(1/1)} + 20\mu_{l'(1/1)})$	$0.168_{(\lambda)}$ $-0.027_{(\rho)}$	
	6P_7		$\frac{1}{105}(3\mu_u + 6\mu_d + \mu_{l(0\otimes 1/\frac{1}{2})} + 2\mu_{l'(0\otimes 1/\frac{1}{2})})$	$0.589_{(\lambda)}$	

TABLE XIII: The excited state magnetic moments of the $P_{\psi}^{\Delta^0}$ states in the diquark-diquark-antiquark model with the 10_f flavor representation. In the λ mode P -wave excitation, $\mu_{l(S_{cd} \otimes S_{ud}/S_{\bar{c}})}$ represents the orbital magnetic moment between \bar{c} and center of mass system of diquark (cd) and diquark (ud), S_{cd} , S_{ud} and $S_{\bar{c}}$ represent the spins of diquark (cd), diquark (ud) and \bar{c} , respectively. $\mu_{l'(S_{cu} \otimes S_{dd}/S_{\bar{c}})}$ represents the orbital magnetic moment between \bar{c} and center of mass system of diquark (cu) and diquark (dd), and S_{cu} , S_{dd} and $S_{\bar{c}}$ represent the spins of diquark (cu), diquark (dd) and \bar{c} , respectively. In the ρ mode P -wave excitation, $\mu_{l(S_{cd}/S_{ud})}$ represents the orbital magnetic moment between diquark (cd) and diquark (ud), S_{cd} and S_{ud} represent the spins of diquark (cd) and diquark (ud), respectively. $\mu_{l'(S_{cu}/S_{dd})}$ represents the orbital magnetic moment between diquark (cu) and diquark (dd), S_{cu} and S_{dd} represent the spins of diquark (cu), diquark (dd), respectively. The $J_1^{P_1} \otimes J_2^{P_2} \otimes J_3^{P_3} \otimes J_4^{P_4}$ are corresponding to the angular momentum and parity of (cq_1), (q_2q_3), \bar{c} and orbital, respectively. The unit is the nuclear magnetic moment μ_N .

$\sqrt{\frac{2}{3}}(cd)\{ud\}\bar{c} + \sqrt{\frac{1}{3}}(cu)\{dd\}\bar{c}$					
J^P	$2s+1L_J$	$J_1^{P_1} \otimes J_2^{P_2} \otimes J_3^{P_3} \otimes J_4^{P_4}$	Expressions	Results	
$\frac{1}{2}^+$	${}^2P_{\frac{1}{2}}$	$(0^+ \otimes 1^+ \otimes \frac{1}{2}^-)_{\frac{1}{2}} \otimes 1^-$	$\frac{1}{27}(-4\mu_u - 8\mu_d - 3\mu_c + 12\mu_{l(0 \otimes 1/\frac{1}{2})} + 6\mu_{l'(0 \otimes 1/\frac{1}{2})})$ $\frac{1}{27}(-4\mu_u - 8\mu_d - 3\mu_c + 12\mu_{l(0/1)} + 6\mu_{l'(0/1)})$	0.360(λ) 0.024(ρ)	
		$((1^+ \otimes 1^+)_{0} \otimes \frac{1}{2}^-)_{\frac{1}{2}} \otimes 1^-$	$\frac{1}{9}(3\mu_c + 4\mu_{l(1 \otimes 1/\frac{1}{2})} + 2\mu_{l'(1 \otimes 1/\frac{1}{2})})$ $\frac{1}{9}(3\mu_c + 4\mu_{l(1/1)} + 2\mu_{l'(1/1)})$	0.529(λ) 0.198(ρ)	
		$((1^+ \otimes 1^+)_{1} \otimes \frac{1}{2}^-)_{\frac{1}{2}} \otimes 1^-$	$\frac{1}{27}(-3\mu_u - 6\mu_d - 6\mu_c + 12\mu_{l(1 \otimes 1/\frac{1}{2})} + 6\mu_{l'(1 \otimes 1/\frac{1}{2})})$ $\frac{1}{27}(-3\mu_u - 6\mu_d - 6\mu_c + 12\mu_{l(1/1)} + 6\mu_{l'(1/1)})$	0.305(λ) -0.027(ρ)	
	${}^4P_{\frac{1}{2}}$	$(0^+ \otimes 1^+ \otimes \frac{1}{2}^-)_{\frac{3}{2}} \otimes 1^-$	$\frac{1}{27}(10\mu_u + 20\mu_d - 15\mu_c - 6\mu_{l(0 \otimes 1/\frac{1}{2})} - 3\mu_{l'(0 \otimes 1/\frac{1}{2})})$ $\frac{1}{27}(10\mu_u + 20\mu_d - 15\mu_c - 6\mu_{l(0/1)} - 3\mu_{l'(0/1)})$	-0.426(λ) -0.259(ρ)	
		$((1^+ \otimes 1^+)_{1} \otimes \frac{1}{2}^-)_{\frac{3}{2}} \otimes 1^-$	$\frac{1}{54}(15\mu_u + 30\mu_d - 15\mu_c - 12\mu_{l(1 \otimes 1/\frac{1}{2})} - 6\mu_{l'(1 \otimes 1/\frac{1}{2})})$ $\frac{1}{54}(15\mu_u + 30\mu_d - 15\mu_c - 12\mu_{l(1/1)} - 6\mu_{l'(1/1)})$	-0.309(λ) -0.144(ρ)	
		$((1^+ \otimes 1^+)_{2} \otimes \frac{1}{2}^-)_{\frac{3}{2}} \otimes 1^-$	$\frac{1}{18}(15\mu_u + 18\mu_d + 15\mu_c - 4\mu_{l(1 \otimes 1/\frac{1}{2})} - 2\mu_{l'(1 \otimes 1/\frac{1}{2})})$ $\frac{1}{18}(15\mu_u + 18\mu_d + 15\mu_c - 4\mu_{l(1/1)} - 2\mu_{l'(1/1)})$	0.140(λ) 0.305(ρ)	
	$\frac{3}{2}^+$	${}^2P_{\frac{3}{2}}$	$(0^+ \otimes 1^+ \otimes \frac{1}{2}^-)_{\frac{1}{2}} \otimes 1^-$	$\frac{1}{9}(4\mu_u + 8\mu_d + 3\mu_c + 6\mu_{l(0 \otimes 1/\frac{1}{2})} + 3\mu_{l'(0 \otimes 1/\frac{1}{2})})$ $\frac{1}{9}(4\mu_u + 8\mu_d + 3\mu_c + 6\mu_{l(0/1)} + 3\mu_{l'(0/1)})$	0.741(λ) 0.238(ρ)
			$((1^+ \otimes 1^+)_{0} \otimes \frac{1}{2}^-)_{\frac{1}{2}} \otimes 1^-$	$\frac{1}{3}(-3\mu_c + 2\mu_{l(1 \otimes 1/\frac{1}{2})} + \mu_{l'(1 \otimes 1/\frac{1}{2})})$ $\frac{1}{3}(-3\mu_c + 2\mu_{l(1/1)} + 1\mu_{l'(1/1)})$	0.186(λ) -0.309(ρ)
			$((1^+ \otimes 1^+)_{1} \otimes \frac{1}{2}^-)_{\frac{1}{2}} \otimes 1^-$	$\frac{1}{9}(3\mu_u + 6\mu_d + 6\mu_c + 6\mu_{l(1 \otimes 1/\frac{1}{2})} + 3\mu_{l'(1 \otimes 1/\frac{1}{2})})$ $\frac{1}{9}(3\mu_u + 6\mu_d + 6\mu_c + 6\mu_{l(1/1)} + 3\mu_{l'(1/1)})$	0.858(λ) 0.364(ρ)
${}^4P_{\frac{3}{2}}$		$(0^+ \otimes 1^+ \otimes \frac{1}{2}^-)_{\frac{3}{2}} \otimes 1^-$	$\frac{1}{45}(22\mu_u + 44\mu_d - 33\mu_c + 12\mu_{l(0 \otimes 1/\frac{1}{2})} + 6\mu_{l'(0 \otimes 1/\frac{1}{2})})$ $\frac{1}{45}(22\mu_u + 44\mu_d - 33\mu_c + 12\mu_{l(0/1)} + 6\mu_{l'(0/1)})$	-0.053(λ) -0.255(ρ)	
		$((1^+ \otimes 1^+)_{1} \otimes \frac{1}{2}^-)_{\frac{3}{2}} \otimes 1^-$	$\frac{1}{90}(33\mu_u + 66\mu_d - 33\mu_c + 24\mu_{l(1 \otimes 1/\frac{1}{2})} + 12\mu_{l'(1 \otimes 1/\frac{1}{2})})$ $\frac{1}{90}(33\mu_u + 66\mu_d - 33\mu_c + 24\mu_{l(1/1)} + 12\mu_{l'(1/1)})$	0.088(λ) -0.110(ρ)	
		$((1^+ \otimes 1^+)_{2} \otimes \frac{1}{2}^-)_{\frac{3}{2}} \otimes 1^-$	$\frac{1}{150}(99\mu_u + 198\mu_d + 165\mu_c + 40\mu_{l(1 \otimes 1/\frac{1}{2})} + 20\mu_{l'(1 \otimes 1/\frac{1}{2})})$ $\frac{1}{150}(99\mu_u + 198\mu_d + 165\mu_c + 40\mu_{l(1/1)} + 20\mu_{l'(1/1)})$	0.679(λ) 0.482(ρ)	
${}^6P_{\frac{3}{2}}$		$((1^+ \otimes 1^+)_{2} \otimes \frac{1}{2}^-)_{\frac{5}{2}} \otimes 1^-$	$\frac{1}{25}(14\mu_u + 42\mu_d - 10\mu_{l(1 \otimes 1/\frac{1}{2})} - 5\mu_{l'(1 \otimes 1/\frac{1}{2})})$ $\frac{1}{25}(14\mu_u + 42\mu_d - 10\mu_{l(1/1)} - 5\mu_{l'(1/1)})$	-0.353(λ) -0.057(ρ)	
$\frac{5}{2}^+$		${}^4P_{\frac{5}{2}}$	$(0^+ \otimes 1^+ \otimes \frac{1}{2}^-) \otimes 1^-$	$\frac{1}{3}(2\mu_u + 4\mu_d - 3\mu_c + 2\mu_{l(0 \otimes 1/\frac{1}{2})} + \mu_{l'(0 \otimes 1/\frac{1}{2})})$ $\frac{1}{3}(2\mu_u + 4\mu_d - 3\mu_c + 2\mu_{l(0/1)} + \mu_{l'(0/1)})$	0.204(λ) -0.300(ρ)
			$((1^+ \otimes 1^+)_{1} \otimes \frac{1}{2}^-)_{\frac{3}{2}} \otimes 1^-$	$\frac{1}{6}(3\mu_u + 6\mu_d - 3\mu_c + 4\mu_{l(1 \otimes 1/\frac{1}{2})} + 2\mu_{l'(1 \otimes 1/\frac{1}{2})})$ $\frac{1}{6}(3\mu_u + 6\mu_d - 3\mu_c + 4\mu_{l(1/1)} + 2\mu_{l'(1/1)})$	0.387(λ) -0.107(ρ)
	$((1^+ \otimes 1^+)_{2} \otimes \frac{1}{2}^-)_{\frac{3}{2}} \otimes 1^-$		$\frac{1}{30}(27\mu_u + 54\mu_d + 15\mu_c + 20\mu_{l(1 \otimes 1/\frac{1}{2})} + 10\mu_{l'(1 \otimes 1/\frac{1}{2})})$ $\frac{1}{30}(27\mu_u + 54\mu_d + 15\mu_c + 20\mu_{l(1/1)} + 10\mu_{l'(1/1)})$	1.194(λ) 0.701(ρ)	
	${}^6P_{\frac{5}{2}}$	$((1^+ \otimes 1^+)_{2} \otimes \frac{1}{2}^-)_{\frac{5}{2}} \otimes 1^-$	$\frac{1}{105}(93\mu_u + 186\mu_d + 20\mu_{l(1 \otimes 1/\frac{1}{2})} + 10\mu_{l'(1 \otimes 1/\frac{1}{2})})$ $\frac{1}{105}(93\mu_u + 186\mu_d + 20\mu_{l(1/1)} + 10\mu_{l'(1/1)})$	0.168(λ) 0.027(ρ)	
	$\frac{7}{2}^+$	6P_7	$((1^+ \otimes 1^+)_{2} \otimes \frac{1}{2}^-)_{\frac{5}{2}} \otimes 1^-$	$\frac{1}{105}(93\mu_u + 186\mu_d + 20\mu_{l(1 \otimes 1/\frac{1}{2})} + 10\mu_{l'(1 \otimes 1/\frac{1}{2})})$ $\frac{1}{105}(93\mu_u + 186\mu_d + 20\mu_{l(1/1)} + 10\mu_{l'(1/1)})$	0.589(λ) 0.027(ρ)

TABLE XIV: The magnetic moments of the $P_{\psi}^{N^0}$ states in the diquark-triquark model with the 8_{1f} and 8_{2f} flavor representation. The $J_1^{P_1} \otimes J_2^{P_2} \otimes J_3^{P_3}$ are corresponding to the angular momentum and parity of triquark, diquark and orbital, respectively. Where the $\mu_{l(S_{\bar{c}ud}/S_{cd})}$ represents the orbital magnetic moment between triquark ($\bar{c}ud$) and diquark (cd), $S_{\bar{c}ud}$ and S_{cd} represent the spins of triquark ($\bar{c}ud$) and diquark (cd), respectively. The $\mu_{l'(S_{\bar{c}dd}/S_{cu})}$ represents the orbital magnetic moment between triquark ($\bar{c}dd$) and diquark (cu), $S_{\bar{c}dd}$ and S_{cu} represent the spins of triquark ($\bar{c}dd$) and diquark (cu), respectively. The unit is the nuclear magnetic moment μ_N .

(cd)(\bar{c} [ud])				
J^P	$2s+1 L_J$	$J_1^{P_1} \otimes J_2^{P_2} \otimes J_3^{P_3}$	Expressions	Results
$\frac{1}{2}^-$	$2S_{\frac{1}{2}}$	$\frac{1}{2}^- \otimes 0^+ \otimes 0^+$	$-\mu_c$	-0.403
		$\frac{1}{2}^- \otimes 1^+ \otimes 0^+$	$\frac{1}{3}(3\mu_c + 2\mu_d)$	-0.228
$\frac{3}{2}^-$	$4S_{\frac{3}{2}}$	$\frac{1}{2}^- \otimes 1^+ \otimes 0^+$	μ_d	-0.947
$\frac{1}{2}^+$	$2P_{\frac{1}{2}}$	$\frac{1}{2}^- \otimes 0^+ \otimes 1^-$	$\frac{1}{3}(\mu_c + 2\mu_{l(\frac{1}{2}/0)})$	0.150
		$(\frac{1}{2}^- \otimes 1^+)_{\frac{1}{2}} \otimes 1^-$	$\frac{1}{9}(-3\mu_c - 2\mu_d + 6\mu_{l(\frac{1}{2}/1)})$	0.087
	$4P_{\frac{1}{2}}$	$(\frac{1}{2}^- \otimes 1^+)_{\frac{3}{2}} \otimes 1^-$	$\frac{1}{9}(5\mu_d - 3\mu_{l(\frac{1}{2}/1)})$	-0.532
$\frac{3}{2}^+$	$2P_{\frac{3}{2}}$	$\frac{1}{2}^- \otimes 0^+ \otimes 1^-$	$-\mu_c + \mu_{l(\frac{1}{2}/0)}$	-0.380
		$(\frac{1}{2}^- \otimes 1^+)_{\frac{1}{2}} \otimes 1^-$	$\frac{1}{3}(3\mu_c + 2\mu_d + 3\mu_{l(\frac{1}{2}/1)})$	-0.212
	$4P_{\frac{3}{2}}$	$(\frac{1}{2}^- \otimes 1^+)_{\frac{3}{2}} \otimes 1^-$	$\frac{1}{15}(11\mu_d + 6\mu_{l(\frac{1}{2}/1)})$	-0.688
$\frac{5}{2}^+$	$4P_{\frac{5}{2}}$	$\frac{1}{2}^- \otimes 1^+ \otimes 1^-$	$\mu_d + \mu_{l(\frac{1}{2}/1)}$	-0.931
$\sqrt{\frac{1}{3}}(cd)(\bar{c}\{ud\}) - \sqrt{\frac{2}{3}}(cu)(\bar{c}\{dd\})$				
J^P	$2s+1 L_J$	$J_1^{P_1} \otimes J_2^{P_2} \otimes J_3^{P_3}$	Expressions	Results
$\frac{1}{2}^-$	$2S_{\frac{1}{2}}$	$\frac{1}{2}^- \otimes 0^+ \otimes 0^+$	$\frac{1}{9}(2\mu_u + 10\mu_d + 3\mu_c)$	-0.497
		$\frac{1}{2}^- \otimes 1^+ \otimes 0^+$	$\frac{1}{27}(10\mu_u - 4\mu_d + 15\mu_c)$	1.066
		$\frac{3}{2}^- \otimes 1^+ \otimes 0^+$	$\frac{1}{27}(-\mu_u + 22\mu_d - 24\mu_c)$	-1.201
$\frac{3}{2}^-$	$4S_{\frac{3}{2}}$	$\frac{1}{2}^- \otimes 1^- \otimes 0^+$	$\frac{1}{9}(8\mu_u + 13\mu_d + 12\mu_c)$	0.854
		$\frac{3}{2}^- \otimes 0^+ \otimes 0^+$	$\frac{1}{3}(\mu_u + 5\mu_d - 3\mu_c)$	-1.351
		$\frac{3}{2}^- \otimes 1^- \otimes 0^+$	$\frac{1}{45}(23\mu_u + 61\mu_d - 15\mu_c)$	-0.450
$\frac{5}{2}^-$	$6S_{\frac{5}{2}}$	$\frac{3}{2}^- \otimes 1^+ \otimes 0^+$	$\mu_u + 2\mu_d$	0
$\frac{1}{2}^+$	$2P_{\frac{1}{2}}$	$\frac{1}{2}^- \otimes 0^+ \otimes 1^-$	$\frac{1}{27}(-2\mu_u - 10\mu_d - 3\mu_c + 6\mu_{l(\frac{1}{2}/0)} + 12\mu_{l'(\frac{1}{2}/0)})$	0.234
		$(\frac{1}{2}^- \otimes 1^+)_{\frac{1}{2}} \otimes 1^-$	$\frac{1}{81}(-10\mu_u + 4\mu_d - 15\mu_c + 18\mu_{l(\frac{1}{2}/1)} + 36\mu_{l'(\frac{1}{2}/1)})$	-0.377
	$4P_{\frac{1}{2}}$	$(\frac{1}{2}^- \otimes 1^+)_{\frac{3}{2}} \otimes 1^-$	$\frac{1}{81}(40\mu_u + 65\mu_d + 60\mu_c - 9\mu_{l(\frac{1}{2}/1)} - 18\mu_{l'(\frac{1}{2}/1)})$	0.286
		$\frac{3}{2}^- \otimes 0^+ \otimes 1^-$	$\frac{1}{27}(5\mu_u + 25\mu_d - 15\mu_c - 3\mu_{l(\frac{3}{2}/0)} - 6\mu_{l'(\frac{3}{2}/0)})$	-0.785
	$2P_{\frac{1}{2}}$	$(\frac{3}{2}^- \otimes 1^+)_{\frac{1}{2}} \otimes 1^-$	$\frac{1}{81}(\mu_u - 22\mu_d + 24\mu_c + 18\mu_{l(\frac{3}{2}/1)} + 36\mu_{l'(\frac{3}{2}/1)})$	0.379
$4P_{\frac{1}{2}}$	$(\frac{3}{2}^- \otimes 1^+)_{\frac{3}{2}} \otimes 1^-$	$\frac{1}{81}(23\mu_u + 61\mu_d - 15\mu_c - 9\mu_{l(\frac{3}{2}/1)} - 18\mu_{l'(\frac{3}{2}/1)})$	-0.240	
$\frac{3}{2}^+$	$2P_{\frac{3}{2}}$	$\frac{1}{2}^- \otimes 0^+ \otimes 1^-$	$\frac{1}{9}(2\mu_u + 10\mu_d + 3\mu_c + 3\mu_{l(\frac{1}{2}/0)} + 6\mu_{l'(\frac{1}{2}/0)})$	-0.395
		$(\frac{1}{2}^- \otimes 1^+)_{\frac{1}{2}} \otimes 1^-$	$\frac{1}{27}(10\mu_u - 4\mu_d + 15\mu_c + 9\mu_{l(\frac{1}{2}/1)} + 18\mu_{l'(\frac{1}{2}/1)})$	1.034
	$4P_{\frac{3}{2}}$	$(\frac{1}{2}^- \otimes 1^+)_{\frac{3}{2}} \otimes 1^-$	$\frac{1}{135}(88\mu_u + 143\mu_d + 132\mu_c + 18\mu_{l(\frac{1}{2}/1)} + 36\mu_{l'(\frac{1}{2}/1)})$	0.613
		$\frac{3}{2}^- \otimes 0^+ \otimes 1^-$	$\frac{1}{45}(11\mu_u + 55\mu_d - 33\mu_c + 6\mu_{l(\frac{3}{2}/0)} + 12\mu_{l'(\frac{3}{2}/0)})$	-0.950
	$2P_{\frac{3}{2}}$	$(\frac{3}{2}^- \otimes 1^+)_{\frac{1}{2}} \otimes 1^-$	$\frac{1}{27}(-\mu_u + 22\mu_d - 24\mu_c + 9\mu_{l(\frac{3}{2}/1)} + 18\mu_{l'(\frac{3}{2}/1)})$	-1.233
$4P_{\frac{3}{2}}$	$(\frac{3}{2}^- \otimes 1^+)_{\frac{3}{2}} \otimes 1^-$	$\frac{1}{675}(253\mu_u + 671\mu_d - 165\mu_c + 90\mu_{l(\frac{3}{2}/1)} + 180\mu_{l'(\frac{3}{2}/1)})$	-0.343	
$6P_{\frac{3}{2}}$	$(\frac{3}{2}^- \otimes 1^+)_{\frac{5}{2}} \otimes 1^-$	$\frac{1}{75}(63\mu_u + 126\mu_d - 15\mu_{l(\frac{3}{2}/1)} - 30\mu_{l'(\frac{3}{2}/1)})$	0.019	
$\frac{5}{2}^+$	$4P_{\frac{5}{2}}$	$\frac{1}{2}^- \otimes 1^+ \otimes 1^-$	$\frac{1}{9}(8\mu_u + 13\mu_d + 12\mu_c + 3\mu_{l(\frac{1}{2}/1)} + 6\mu_{l'(\frac{1}{2}/1)})$	0.822
		$\frac{3}{2}^- \otimes 0^+ \otimes 1^-$	$\frac{1}{3}(\mu_u + 5\mu_d - 3\mu_c + \mu_{l(\frac{3}{2}/0)} + 2\mu_{l'(\frac{3}{2}/0)})$	-1.248
		$(\frac{3}{2}^- \otimes 1^+)_{\frac{3}{2}} \otimes 1^-$	$\frac{1}{45}(23\mu_u + 61\mu_d - 15\mu_c + 15\mu_{l(\frac{3}{2}/1)} + 30\mu_{l'(\frac{3}{2}/1)})$	-0.482
	$6P_{\frac{5}{2}}$	$(\frac{3}{2}^- \otimes 1^+)_{\frac{5}{2}} \otimes 1^-$	$\frac{1}{105}(93\mu_u + 186\mu_d + 10\mu_{l(\frac{3}{2}/1)} + 20\mu_{l'(\frac{3}{2}/1)})$	-0.009

TABLE XV: The magnetic moments of the $P_\psi^{\Delta 0}$ states in the diquark-triquark model with the 10_f flavor representation. The $J_1^{P_1} \otimes J_2^{P_2} \otimes J_3^{P_3}$ are corresponding to the angular momentum and parity of triquark, diquark and orbital, respectively. Where the $\mu_{l(S_{\bar{c}ud}/S_{cd})}$ represents the orbital magnetic moment between triquark ($\bar{c}ud$) and diquark (cd), $S_{\bar{c}ud}$ and S_{cd} represent the spins of triquark ($\bar{c}ud$) and diquark (cd), respectively. The $\mu_{l'(S_{\bar{c}dd}/S_{cu})}$ represents the orbital magnetic moment between triquark ($\bar{c}dd$) and diquark (cu), $S_{\bar{c}dd}$ and S_{cu} represent the spins of triquark ($\bar{c}dd$) and diquark (cu), respectively. The unit is the nuclear magnetic moment μ_N .

$\sqrt{\frac{2}{3}}(cd)(\bar{c}\{ud\}) + \sqrt{\frac{1}{3}}(cu)(\bar{c}\{dd\})$				
J^P	$2s+1L_J$	$J_1^{P_1} \otimes J_2^{P_2} \otimes J_3^{P_3}$	Expressions	Results
$\frac{1}{2}^-$	$2S_{\frac{1}{2}}$	$\frac{1}{2}^- \otimes 0^+ \otimes 0^+$	$\frac{1}{9}(4\mu_u + 8\mu_d + 3\mu_c)$	0.134
		$\frac{1}{2}^- \otimes 1^+ \otimes 0^+$	$\frac{1}{27}(2\mu_u + 4\mu_d + 15\mu_c)$	0.224
		$\frac{3}{2}^- \otimes 1^+ \otimes 0^+$	$\frac{1}{27}(7\mu_u + 14\mu_d - 24\mu_c)$	-0.359
$\frac{3}{2}^-$	$4S_{\frac{3}{2}}$	$\frac{1}{2}^- \otimes 1^- \otimes 0^+$	$\frac{1}{9}(7\mu_u + 14\mu_d + 12\mu_c)$	0.539
		$\frac{3}{2}^- \otimes 0^+ \otimes 0^+$	$\frac{1}{3}(2\mu_u + 4\mu_d - 3\mu_c)$	-0.403
		$\frac{3}{2}^- \otimes 1^- \otimes 0^+$	$\frac{1}{45}(28\mu_u + 56\mu_d - 15\mu_c)$	-0.134
$\frac{5}{2}^-$	$6S_{\frac{5}{2}}$	$\frac{3}{2}^- \otimes 1^+ \otimes 0^+$	$\mu_u + 2\mu_d$	0
$\frac{1}{2}^+$	$2P_{\frac{1}{2}}$	$\frac{1}{2}^- \otimes 0^+ \otimes 1^-$	$\frac{1}{27}(-4\mu_u - 8\mu_d - 3\mu_c + 12\mu_{l(\frac{1}{2}/0)} + 6\mu_{l'(\frac{1}{2}/0)})$	0.001
		$(\frac{1}{2}^- \otimes 1^+)_{\frac{1}{2}} \otimes 1^-$	$\frac{1}{81}(-2\mu_u - 4\mu_d - 15\mu_c + 36\mu_{l(\frac{1}{2}/1)} + 18\mu_{l'(\frac{1}{2}/1)})$	-0.059
	$4P_{\frac{1}{2}}$	$(\frac{1}{2}^- \otimes 1^+)_{\frac{3}{2}} \otimes 1^-$	$\frac{1}{81}(35\mu_u + 70\mu_d + 60\mu_c - 18\mu_{l(\frac{1}{2}/1)} - 9\mu_{l'(\frac{1}{2}/1)})$	0.191
		$\frac{3}{2}^- \otimes 0^+ \otimes 1^-$	$\frac{1}{27}(10\mu_u + 20\mu_d - 15\mu_c - 6\mu_{l(\frac{3}{2}/0)} - 3\mu_{l'(\frac{3}{2}/0)})$	-0.247
$\frac{3}{2}^+$	$2P_{\frac{3}{2}}$	$(\frac{3}{2}^- \otimes 1^+)_{\frac{1}{2}} \otimes 1^-$	$\frac{1}{81}(-7\mu_u - 14\mu_d + 24\mu_c + 36\mu_{l(\frac{3}{2}/1)} + 18\mu_{l'(\frac{3}{2}/1)})$	0.136
		$(\frac{3}{2}^- \otimes 1^+)_{\frac{3}{2}} \otimes 1^-$	$\frac{1}{81}(28\mu_u + 56\mu_d - 15\mu_c - 18\mu_{l(\frac{3}{2}/1)} - 9\mu_{l'(\frac{3}{2}/1)})$	-0.083
$\frac{3}{2}^+$	$2P_{\frac{3}{2}}$	$\frac{1}{2}^- \otimes 0^+ \otimes 1^-$	$\frac{1}{9}(4\mu_u + 8\mu_d + 3\mu_c + 6\mu_{l(\frac{1}{2}/0)} + 3\mu_{l'(\frac{1}{2}/0)})$	0.162
		$(\frac{1}{2}^- \otimes 1^+)_{\frac{1}{2}} \otimes 1^-$	$\frac{1}{27}(2\mu_u + 4\mu_d + 15\mu_c + 18\mu_{l(\frac{1}{2}/1)} + 9\mu_{l'(\frac{1}{2}/1)})$	0.248
	$4P_{\frac{3}{2}}$	$(\frac{1}{2}^- \otimes 1^+)_{\frac{3}{2}} \otimes 1^-$	$\frac{1}{135}(77\mu_u + 154\mu_d + 132\mu_c + 36\mu_{l(\frac{1}{2}/1)} + 18\mu_{l'(\frac{1}{2}/1)})$	0.404
		$\frac{3}{2}^- \otimes 0^+ \otimes 1^-$	$\frac{1}{45}(22\mu_u + 44\mu_d - 33\mu_c + 12\mu_{l(\frac{3}{2}/0)} + 6\mu_{l'(\frac{3}{2}/0)})$	-0.269
	$2P_{\frac{3}{2}}$	$(\frac{3}{2}^- \otimes 1^+)_{\frac{1}{2}} \otimes 1^-$	$\frac{1}{27}(7\mu_u + 14\mu_d - 24\mu_c + 18\mu_{l(\frac{3}{2}/1)} + 9\mu_{l'(\frac{3}{2}/1)})$	-0.335
$4P_{\frac{3}{2}}$		$(\frac{3}{2}^- \otimes 1^+)_{\frac{3}{2}} \otimes 1^-$	$\frac{1}{675}(308\mu_u + 616\mu_d - 165\mu_c + 180\mu_{l(\frac{3}{2}/1)} + 90\mu_{l'(\frac{3}{2}/1)})$	-0.089
		$(\frac{3}{2}^- \otimes 1^+)_{\frac{5}{2}} \otimes 1^-$	$\frac{1}{75}(63\mu_u + 126\mu_d - 30\mu_{l(\frac{3}{2}/1)} - 15\mu_{l'(\frac{3}{2}/1)})$	-0.014
$\frac{5}{2}^+$	$4P_{\frac{5}{2}}$	$\frac{1}{2}^- \otimes 1^+ \otimes 1^-$	$\frac{1}{9}(7\mu_u + 14\mu_d + 12\mu_c + 6\mu_{l(\frac{1}{2}/1)} + 3\mu_{l'(\frac{1}{2}/1)})$	0.562
		$\frac{3}{2}^- \otimes 0^+ \otimes 1^-$	$\frac{1}{3}(2\mu_u + 4\mu_d - 3\mu_c + 2\mu_{l(\frac{3}{2}/0)} + \mu_{l'(\frac{3}{2}/0)})$	-0.335
		$(\frac{3}{2}^- \otimes 1^+)_{\frac{3}{2}} \otimes 1^-$	$\frac{1}{45}(28\mu_u + 56\mu_d - 15\mu_c + 30\mu_{l(\frac{3}{2}/1)} + 15\mu_{l'(\frac{3}{2}/1)})$	-0.110
$\frac{7}{2}^+$	$6P_{\frac{7}{2}}$	$(\frac{3}{2}^- \otimes 1^+)_{\frac{5}{2}} \otimes 1^-$	$\frac{1}{105}(93\mu_u + 186\mu_d + 20\mu_{l(\frac{3}{2}/1)} + 10\mu_{l'(\frac{3}{2}/1)})$	0.007
		$\frac{3}{2}^- \otimes 1^+ \otimes 1^-$	$\frac{1}{3}(3\mu_u + 6\mu_d + 2\mu_{l(\frac{3}{2}/1)} + \mu_{l'(\frac{3}{2}/1)})$	0.024

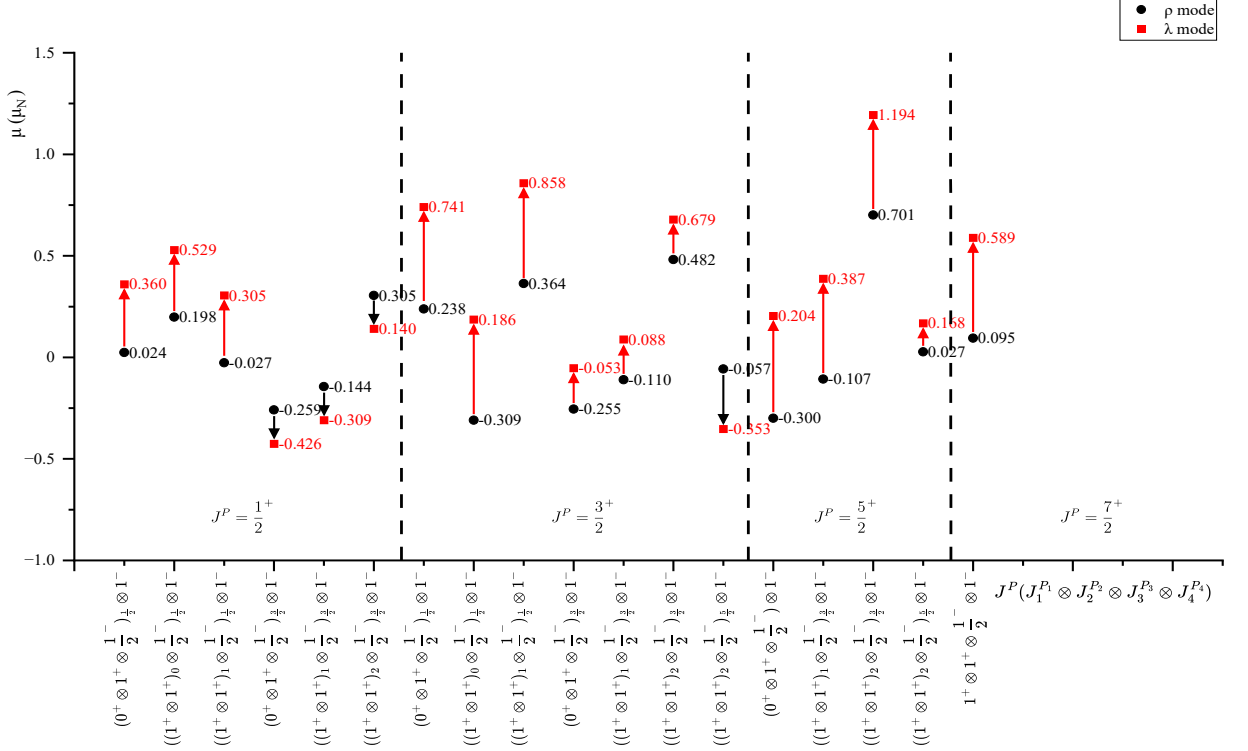


FIG. 2: The excited state magnetic moments of the $P_\psi^{\Delta^0}$ states in the diquark-diquark-antiquark model with the 10_f flavor representation. Here, the red arrow represents the magnetic moments of the λ excitation state are larger than the magnetic moments of the ρ excitation state, and the black arrow represents the magnetic moments of the ρ excitation state are larger than the magnetic moments of the λ excitation state.

$J_4^{P_4} = 1^+ \otimes 1^+ \otimes \frac{1}{2}^- \otimes 0^+$. In Table XII and Table XIII, the magnetic moment expressions of λ excitation $P_\psi^{N^0}$ states with 8_{1f} flavor representation and λ excitation $P_\psi^{\Delta^0}$ states with 10_f flavor representation are equal whose spin configurations satisfying $J_1^{P_1} \otimes J_2^{P_2} \otimes J_3^{P_3} \otimes J_4^{P_4} = 1^+ \otimes 1^+ \otimes \frac{1}{2}^- \otimes 1^-$. In the magnetic moment expression of λ excitation $P_\psi^{N^0}$ states and $P_\psi^{\Delta^0}$ states, the orbital magnetic moment $\mu_{l(1 \otimes 1/2)} = \mu_{l'(1 \otimes 1/2)}$, when we assume exact isospin symmetry with $m_u = m_d$. For example, in Table X, the hidden-charm pentaquark states wave function $\sqrt{\frac{1}{3}}(cd)\{ud\}\bar{c} - \sqrt{\frac{2}{3}}(cu)\{dd\}\bar{c}$ and $\sqrt{\frac{2}{3}}(cd)\{ud\}\bar{c} + \sqrt{\frac{1}{3}}(cu)\{dd\}\bar{c}$ with $J^P = \frac{3}{2}^-$ has spin configurations $(1^+ \otimes 1^+)_{2} \otimes \frac{1}{2}^- \otimes 0^+$, and their magnetic moments are all $0.605\mu_N$. In Table XII and Table XIII, the magnetic moments of the hidden-charm pentaquark states with $J^P = \frac{7}{2}^+$ are both $0.589\mu_N$, and their corresponding spin configurations are $1^+ \otimes 1^+ \otimes \frac{1}{2}^- \otimes 1^-$.

- In Table III, the hidden-charm pentaquark states wave function $\sqrt{\frac{2}{3}}|\Sigma_c^+ D^{*-}\rangle + \sqrt{\frac{1}{3}}|\Sigma_c^0 \bar{D}^{*0}\rangle$ with $J^P = \frac{1}{2}^+$ has spin configurations $(\frac{1}{2}^+ \otimes 1^-)_{\frac{1}{2}} \otimes 1^-$ and $(\frac{1}{2}^+ \otimes 1^-)_{\frac{3}{2}} \otimes$

1^- in the P -wave excitation. Their magnetic moments are $0.037\mu_N$ and $-0.280\mu_N$, respectively. The magnetic moments of the same quantum numbers and quark configurations of the pentaquark states exist obvious differences, indicating that the magnetic moments can indeed distinguish the inner structures of the pentaquark states.

- When the S -wave pentaquark has the highest spin $S = \frac{5}{2}$, the three models give the same magnetic moment $\mu_u + 2\mu_d$. If we use $m_u = m_d$, one gets a vanishing number. The reason for the same result in different models is that magnetic moment is only related with spin structure (of course it is affected by the flavor and color structures). The highest-spin case means that any two quarks are in the $S = 1$ state. In the considered three models, $J^P = \frac{5}{2}^-$ states exist in 8_f and 10_f flavor representations, which means that at least one qq is in the $I = 1$, $S = 1$, and $\bar{3}_c$ state. To form a colorless pentaquark, cq may be both 6_c and $\bar{3}_c$, but only $\bar{3}_c$ is possible from the model assumptions. Therefore, the color-spin structures for the highest-spin pentaquark in the three models are

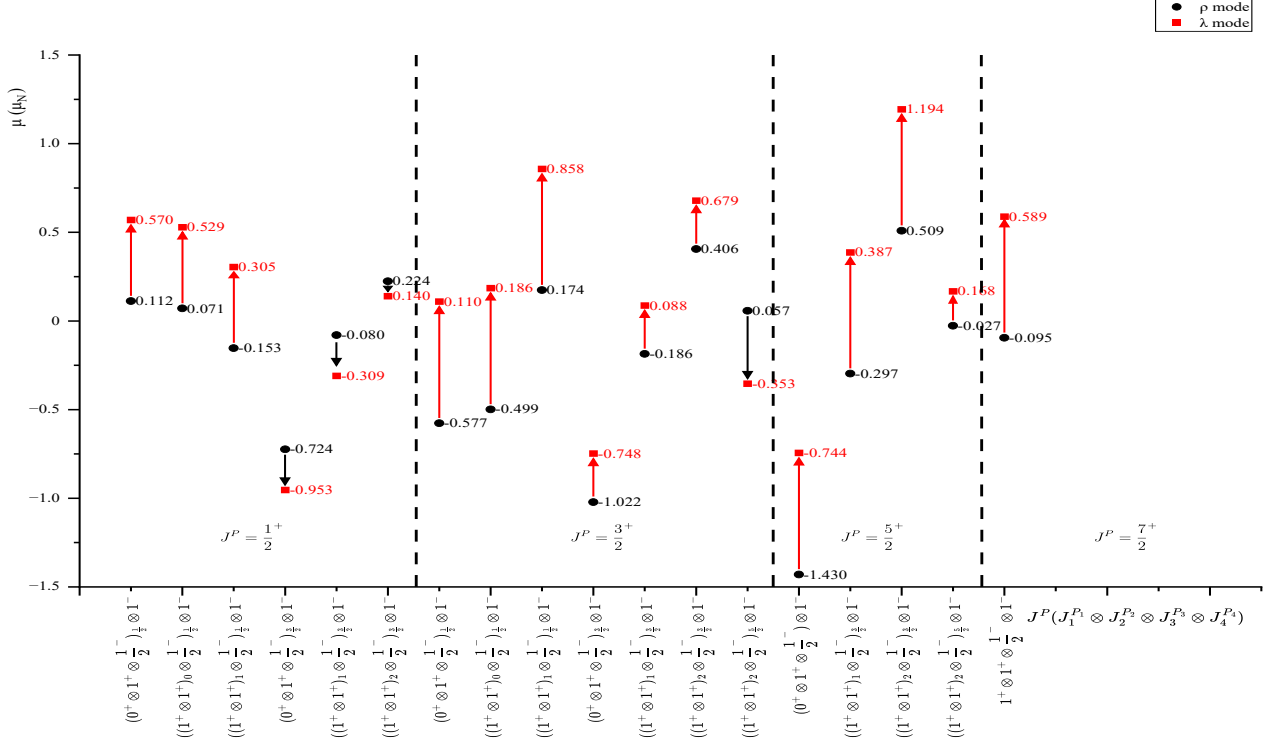


FIG. 3: The excited state magnetic moments of the P_ψ^{N0} states in the diquark-diquark-antiquark model with the 8_{1f} flavor representation. Here, the red arrow represents the magnetic moments of the λ excitation state are larger than the magnetic moments of the ρ excitation state, and the black arrow represents the magnetic moments of the ρ excitation state are larger than the magnetic moments of the λ excitation state.

the same and thus the resulting magnetic moments are the same.

B. Transition magnetic moments of the P_ψ^{N0} states and $P_\psi^{\Delta 0}$ states in the molecular model

We study the transition magnetic moment of the P_ψ^{N0} states and $P_\psi^{\Delta 0}$ states in the molecular model. Comparing the data, we obtain the following interesting points.

- There is an obvious rule between the expressions of transition magnetic moments with the 8_{1f} and 10_f flavor representation. In Table VII and Table IX, the transition magnetic moment expression of $\Sigma_c \bar{D}^{(*)} | \frac{1}{2}^- \rangle \rightarrow \Sigma_c \bar{D} | \frac{1}{2}^- \rangle \gamma$ process are in the form of $k(\mu_{D^{*-} \rightarrow D^-} + 2\mu_{\bar{D}^{*0} \rightarrow \bar{D}^0})$ with 8_{1f} flavor representation and $k(2\mu_{D^{*-} \rightarrow D^-} + \mu_{\bar{D}^{*0} \rightarrow \bar{D}^0})$ with 10_f flavor representation. Here, k is a real number.

- The transition magnetic moment of hidden-charm molecular pentaquark can be expressed as a linear combination of transition magnetic moments or magnetic

moments. In Table VII, the transition magnetic moment of the $\Sigma_c \bar{D}^{*} | \frac{1}{2}^- \rangle \rightarrow \Sigma_c \bar{D} | \frac{1}{2}^- \rangle \gamma$ process is related to the transition magnetic moment of the $\mu_{D^{*-} \rightarrow D^-}$ and $\mu_{\bar{D}^{*0} \rightarrow \bar{D}^0}$. The transition magnetic moment of the $\Sigma_c^* \bar{D}^{*} | \frac{3}{2}^- \rangle \rightarrow \Sigma_c^* \bar{D}^{*} | \frac{3}{2}^- \rangle \gamma$ process can be expressed as a linear combination of magnetic moments $\mu_{\Sigma_c^{*+}}$, $\mu_{\Sigma_c^{*0}}$, $\mu_{D^{*-}}$ and $\mu_{\bar{D}^{*0}}$.

- The transition process is different due to different hadron states corresponding to the flavor wave functions. For example, Table VII lists the transition magnetic moments of S -wave $\Sigma_c^{(*)} \bar{D}^{(*)}$ -type hidden-charm molecular pentaquarks between 8_{1f} states, Table VIII lists the transition magnetic moments of S -wave $\Lambda_c D^{(*)}$ -type hidden-charm molecular pentaquarks between 8_{2f} states.

VII. SUMMARY

In recent years, the study of pentaquark states has made continuous breakthroughs. Inspired by the discovery of the P_ψ^{N+} states, we believe that the discovery of

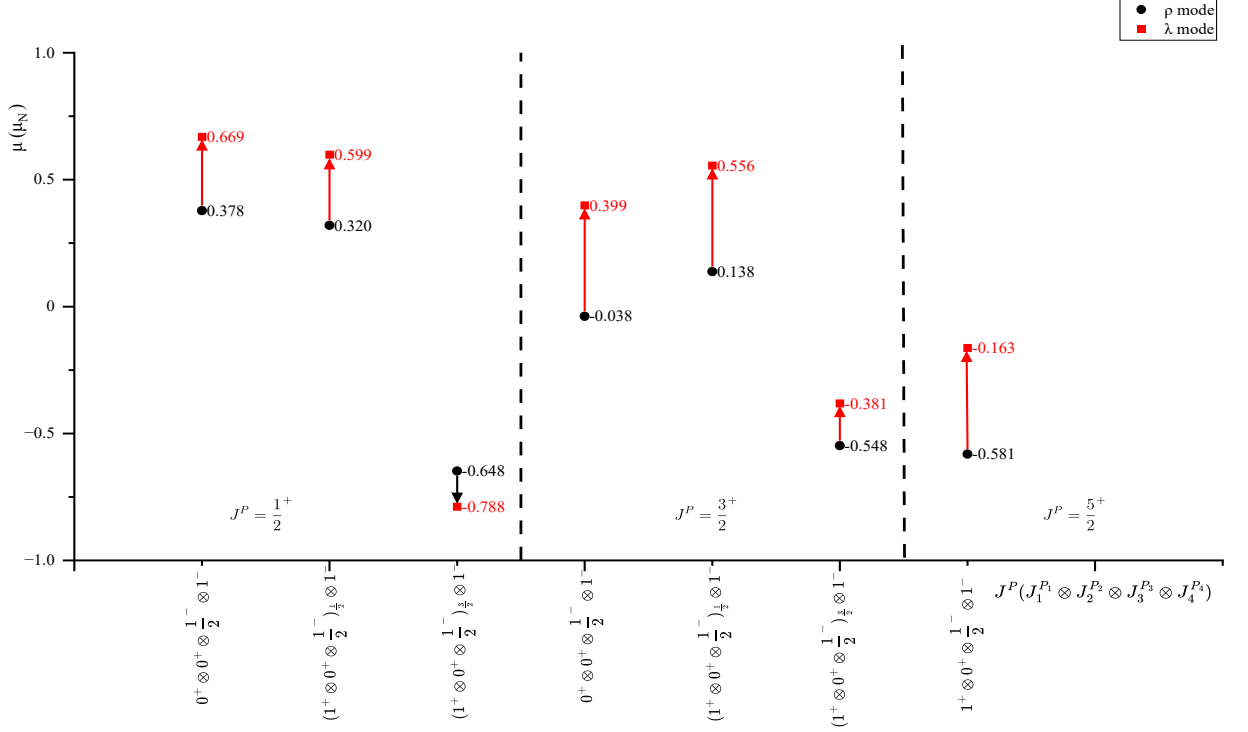


FIG. 4: The excited state magnetic moments of the $P_\psi^{N^0}$ states in the diquark-diquark-antiquark model with the 8_{2f} flavor representation. Here, the red arrow represents the magnetic moments of the λ excitation state are larger than the magnetic moments of the ρ excitation state, and the black arrow represents the magnetic moments of the ρ excitation state are larger than the magnetic moments of the λ excitation state.

the $P_\psi^{N^0}$ states and $P_\psi^{\Delta^0}$ states is inevitable over time. At present, the study of strange hadron states has attracted extensive attention in both experiment and theory, but the study of their magnetic moments and transition magnetic moments has not received enough attention. Magnetic moment is an inherent attribute of particles. The magnetic moment and transition magnetic moment can provide very useful clues for studying the internal structure of strange hadrons.

In this work, we construct the flavor wave functions of the $P_\psi^{N^0}$ states and $P_\psi^{\Delta^0}$ states in the molecular model, the diquark-diquark-antiquark model and the diquark-triquark, and discuss their color configurations. We systematically calculate the magnetic moments and transition magnetic moments of the $P_\psi^{N^0}$ states and $P_\psi^{\Delta^0}$ states, and simply calculated the magnetic moments and transition magnetic moments of $P_\psi^{\Delta^{++}}$ states and $P_\psi^{\Delta^-}$ states in the molecular model that have not yet been explored (see the Appendix A). The results clearly show that the flavor-spin wave function fundamentally determines the

magnetic moment and the transition magnetic moment. The flavor-spin wave functions of different initial and final states determines the difference of transition magnetic moment. The same spin configuration has different magnetic moments in different models, and the different spin configuration has different magnetic moments in same models. The different flavor-spin compositions of pentaquark states contain important information about their internal structure. Therefore, this work will provide important data support for us to explore the inner structures of the hidden-charm pentaquark states. At present, for the calculation of transition magnetic moments, we only consider molecular model. The molecular model is the mainstream model for studying the transition magnetic moment of pentaquark states, which includes two parts: baryons and mesons, making it easy to visually analyze its results. Calculating the transition magnetic moments of other models requires recombining the relevant flavor-spin wave function, which will be discussed in our future work.

ACKNOWLEDGMENTS

This project is supported by the National Natural Science Foundation of China under Grants No. 11905171, No. 12047502 and No. 12247103. This work is also supported by the Natural Science Basic Research Plan in Shaanxi Province of China (Grant No. 2022JQ-025) and Shaanxi Fundamental Science Research Project for Mathematics and Physics (Grant No.22JSQ016).

Appendix A: MAGNETIC MOMENTS AND TRANSITION MAGNETIC MOMENTS OF THE $P_\psi^{\Delta^{++}}$ STATES AND THE $P_\psi^{\Delta^-}$ STATES IN THE MOLECULAR MODEL

In this section, we briefly supplement the unexplored magnetic moments and transition magnetic moments of $P_\psi^{\Delta^{++}}$ states and $P_\psi^{\Delta^-}$ states in the molecular model. The flavor wave function of $P_\psi^{\Delta^{++}}$ states and $P_\psi^{\Delta^-}$ states in the molecular model is 10_f flavor representation.

$$P_\psi^{\Delta^{++}} : \left| \Sigma_c^{(*)++} \bar{D}^{(*)0} \right\rangle, \quad (\text{A1})$$

$$P_\psi^{\Delta^-} : \left| \Sigma_c^{(*)0} D^{(*)-} \right\rangle. \quad (\text{A2})$$

The spin wave functions of $P_\psi^{\Delta^{++}}$ states and $P_\psi^{\Delta^-}$ states with the same spin configuration are the same, and here we list the spin wave functions of $P_\psi^{\Delta^{++}}$ states.

$$\begin{aligned} |S, S_z\rangle = & \\ & \sum_{S'_{\Sigma_c^{(*)}}, S'_{\bar{D}^{(*)}}} C_{S_{\Sigma_c^{(*)}} S'_{\Sigma_c^{(*)}}, S_{\bar{D}^{(*)}} S'_{\bar{D}^{(*)}}}^{S, S_z} \left| S_{\Sigma_c^{(*)}}, S'_{\Sigma_c^{(*)}} \right\rangle \left| S_{\bar{D}^{(*)}}, S'_{\bar{D}^{(*)}} \right\rangle. \end{aligned} \quad (\text{A3})$$

Here, S and S_z represent the spin and the spin third components of $P_\psi^{\Delta^{++}}$ states. The $S_{\Sigma_c^{(*)}}$, $S_{\bar{D}^{(*)}}$ are spin of $\Sigma_c^{(*)}$ and $\bar{D}^{(*)}$, respectively. The $S'_{\Sigma_c^{(*)}}$, $S'_{\bar{D}^{(*)}}$ are spin third component of $\Sigma_c^{(*)}$ and $\bar{D}^{(*)}$, respectively.

The magnetic moments and transition magnetic moments of $P_\psi^{\Delta^{++}}$ states in the molecular model are presented in Table XVI and Table XVIII, respectively. The transition magnetic moments of the $\Sigma_c^* \bar{D}^* |^2 S_{1/2}\rangle \rightarrow \Sigma_c \bar{D}^* |^2 S_{1/2}\rangle_\gamma$ and $\Sigma_c^* \bar{D}^* |^6 S_{5/2}\rangle \rightarrow \Sigma_c \bar{D}^* |^2 S_{1/2}\rangle_\gamma$ processes in $P_\psi^{\Delta^{++}}$ states are zero. The magnetic moments and transition magnetic moments of $P_\psi^{\Delta^-}$ states in the molecular model are presented in Table XVII and Table XIX, respectively. The transition magnetic moments of the $\Sigma_c^* D^* |^2 S_{1/2}\rangle \rightarrow \Sigma_c D^* |^2 S_{1/2}\rangle_\gamma$ and $\Sigma_c^* D^* |^6 S_{5/2}\rangle \rightarrow \Sigma_c D^* |^2 S_{1/2}\rangle_\gamma$ processes in $P_\psi^{\Delta^-}$ states are zero.

-
- [1] M. Gell-Mann, ‘‘A Schematic Model of Baryons and Mesons,’’ *Phys. Lett.* **8**, 214-215 (1964).
 - [2] G. Zweig, ‘‘An SU(3) model for strong interaction symmetry and its breaking. Version 1,’’ CERN-TH-401.
 - [3] S. K. Choi *et al.* [Belle], ‘‘Observation of a narrow charmonium-like state in exclusive $B^\pm \rightarrow K^\pm \pi^+ \pi^- J/\psi$ decays,’’ *Phys. Rev. Lett.* **91**, 262001 (2003).
 - [4] K. Abe *et al.* [Belle], ‘‘Observation of a near-threshold omega J/psi mass enhancement in exclusive $B \rightarrow K$ omega J/psi decays,’’ *Phys. Rev. Lett.* **94**, 182002 (2005).
 - [5] R. Mizuk *et al.* [Belle], ‘‘Observation of two resonance-like structures in the pi+ chi(c1) mass distribution in exclusive anti-B0 \rightarrow K- pi+ chi(c1) decays,’’ *Phys. Rev. D* **78**, 072004 (2008).
 - [6] T. Aaltonen *et al.* [CDF], ‘‘Evidence for a Narrow Near-Threshold Structure in the $J/\psi\phi$ Mass Spectrum in $B^+ \rightarrow J/\psi\phi K^+$ Decays,’’ *Phys. Rev. Lett.* **102**, 242002 (2009).
 - [7] R. Aaij *et al.* [LHCb], ‘‘Observation of the resonant character of the $Z(4430)^-$ state,’’ *Phys. Rev. Lett.* **112**, no.22, 222002 (2014).
 - [8] R. Aaij *et al.* [LHCb], ‘‘Observation of $J/\psi\phi$ structures consistent with exotic states from amplitude analysis of $B^+ \rightarrow J/\psi\phi K^+$ decays,’’ *Phys. Rev. Lett.* **118**, no.2, 022003 (2017).
 - [9] R. Aaij *et al.* [LHCb], ‘‘Evidence for an $\eta_c(1S)\pi^-$ resonance in $B^0 \rightarrow \eta_c(1S)K^+\pi^-$ decays,’’ *Eur. Phys. J. C* **78**, no.12, 1019 (2018).
 - [10] B. Aubert *et al.* [BaBar], ‘‘Observation of a broad structure in the $\pi^+\pi^- J/\psi$ mass spectrum around 4.26-GeV/c²,’’ *Phys. Rev. Lett.* **95**, 142001 (2005).
 - [11] C. Z. Yuan *et al.* [Belle], ‘‘Measurement of e+ e- \rightarrow pi+ pi- J/psi cross-section via initial state radiation at Belle,’’ *Phys. Rev. Lett.* **99**, 182004 (2007).
 - [12] X. L. Wang *et al.* [Belle], ‘‘Observation of Two Resonant Structures in e+e- to pi+ pi- psi(2S) via Initial State Radiation at Belle,’’ *Phys. Rev. Lett.* **99**, 142002 (2007).
 - [13] G. Pakhlova *et al.* [Belle], ‘‘Observation of a near-threshold enhancement in the e+e- \rightarrow Lambda+(c) Lambda-(c) cross section using initial-state radiation,’’ *Phys. Rev. Lett.* **101**, 172001 (2008).
 - [14] M. Ablikim *et al.* [BESIII], ‘‘Evidence of Two Resonant Structures in $e^+e^- \rightarrow \pi^+\pi^- h_c$,’’ *Phys. Rev. Lett.* **118**, no.9, 092002 (2017).
 - [15] R. Aaij *et al.* [LHCb], ‘‘Observation of $J/\psi\phi$ Resonances Consistent with Pentaquark States in $\Lambda_b^0 \rightarrow J/\psi K^- p$

TABLE XVI: The magnetic moments of the $P_\psi^{\Delta^{++}}$ states in the molecular model with the 10_f flavor representation. The $J_1^{P_1} \otimes J_2^{P_2} \otimes J_3^{P_3}$ are corresponding to the angular momentum and parity of baryon, meson and orbital, respectively. The $\mu_{l(\text{baryon/meson})}$ represents the orbital excitation between corresponding hadrons. The unit is the nuclear magnetic moment μ_N .

$ \Sigma_c^{(*)++} \bar{D}^{(*)0}\rangle$				
J^P	$^{2s+1}L_J$	$J_1^{P_1} \otimes J_2^{P_2} \otimes J_3^{P_3}$	Expressions	Results
$\frac{1}{2}^-$	$^2S_{\frac{1}{2}}$	$\frac{1}{2}^+ \otimes 0^- \otimes 0^+$	$\frac{1}{3} (4\mu_u - \mu_c)$	2.392
		$\frac{1}{2}^+ \otimes 1^- \otimes 0^+$	$\frac{1}{9} (2\mu_u - 5\mu_c)$	0.197
		$\frac{3}{2}^+ \otimes 1^- \otimes 0^+$	$\frac{1}{9} (7\mu_u + 8\mu_c)$	1.832
$\frac{3}{2}^-$	$^4S_{\frac{3}{2}}$	$\frac{1}{2}^+ \otimes 1^- \otimes 0^+$	$\frac{1}{3} (7\mu_u - 4\mu_c)$	3.884
		$\frac{3}{2}^+ \otimes 0^- \otimes 0^+$	$2\mu_u + \mu_c$	4.193
		$\frac{3}{2}^+ \otimes 1^- \otimes 0^+$	$\frac{1}{15} (28\mu_u + 5\mu_c)$	3.672
$\frac{5}{2}^-$	$^6S_{\frac{5}{2}}$	$\frac{3}{2}^+ \otimes 1^- \otimes 0^+$	$3\mu_u$	5.685
$\frac{1}{2}^+$	$^2P_{\frac{1}{2}}$	$\frac{1}{2}^+ \otimes 0^- \otimes 1^-$	$\frac{1}{9} (-4\mu_u + \mu_c + 6\mu_{l(\Sigma_c^+ + \bar{D}^0)})$	-0.577
		$(\frac{1}{2}^+ \otimes 1^-)_{\frac{1}{2}} \otimes 1^-$	$\frac{1}{27} (-2\mu_u + 5\mu_c + 18\mu_{l(\Sigma_c^+ + \bar{D}^0)})$	0.164
	$^4P_{\frac{1}{2}}$	$(\frac{1}{2}^+ \otimes 1^-)_{\frac{3}{2}} \otimes 1^-$	$\frac{1}{27} (35\mu_u - 20\mu_c - 9\mu_{l(\Sigma_c^+ + \bar{D}^0)})$	2.043
		$\frac{3}{2}^+ \otimes 0^- \otimes 1^-$	$\frac{1}{9} (10\mu_u + 5\mu_c - 3\mu_{l(\Sigma_c^{*++} + \bar{D}^0)})$	2.224
	$^2P_{\frac{1}{2}}$	$(\frac{3}{2}^+ \otimes 1^-)_{\frac{1}{2}} \otimes 1^-$	$\frac{1}{27} (-7\mu_u - 8\mu_c + 18\mu_{l(\Sigma_c^* + \bar{D}^0)})$	-0.391
$^4P_{\frac{1}{2}}$	$(\frac{3}{2}^+ \otimes 1^-)_{\frac{3}{2}} \otimes 1^-$	$\frac{1}{27} (28\mu_u + 5\mu_c - 9\mu_{l(\Sigma_c^{*++} + \bar{D}^0)})$	1.930	
$\frac{3}{2}^+$	$^2P_{\frac{3}{2}}$	$\frac{1}{2}^+ \otimes 0^- \otimes 1^-$	$\frac{1}{3} (4\mu_u - \mu_c + 3\mu_{l(\Sigma_c^+ + \bar{D}^0)})$	2.722
		$(\frac{1}{2}^+ \otimes 1^-)_{\frac{1}{2}} \otimes 1^-$	$\frac{1}{9} (2\mu_u - 5\mu_c + 9\mu_{l(\Sigma_c^+ + \bar{D}^0)})$	0.541
	$^4P_{\frac{3}{2}}$	$(\frac{1}{2}^+ \otimes 1^-)_{\frac{3}{2}} \otimes 1^-$	$\frac{1}{45} (77\mu_u - 44\mu_c + 18\mu_{l(\Sigma_c^+ + \bar{D}^0)})$	2.986
		$\frac{3}{2}^+ \otimes 0^- \otimes 1^-$	$\frac{1}{15} (22\mu_u + 11\mu_c + 6\mu_{l(\Sigma_c^{*++} + \bar{D}^0)})$	3.202
	$^2P_{\frac{3}{2}}$	$(\frac{3}{2}^+ \otimes 1^-)_{\frac{1}{2}} \otimes 1^-$	$\frac{1}{9} (7\mu_u + 8\mu_c + 9\mu_{l(\Sigma_c^* + \bar{D}^0)})$	2.163
	$^4P_{\frac{3}{2}}$	$(\frac{3}{2}^+ \otimes 1^-)_{\frac{3}{2}} \otimes 1^-$	$\frac{1}{225} (308\mu_u + 55\mu_c + 90\mu_{l(\Sigma_c^{*++} + \bar{D}^0)})$	2.825
$^6P_{\frac{3}{2}}$	$(\frac{3}{2}^+ \otimes 1^-)_{\frac{5}{2}} \otimes 1^-$	$\frac{1}{25} (63\mu_u - 15\mu_{l(\Sigma_c^{*++} + \bar{D}^0)})$	4.577	
$\frac{5}{2}^+$	$^4P_{\frac{5}{2}}$	$\frac{1}{2}^+ \otimes 1^- \otimes 1^-$	$\frac{1}{3} (7\mu_u - 4\mu_c + 3\mu_{l(\Sigma_c^+ + \bar{D}^0)})$	4.228
		$\frac{3}{2}^+ \otimes 0^- \otimes 1^-$	$2\mu_u + \mu_c + \mu_{l(\Sigma_c^{*++} + \bar{D}^0)}$	4.510
		$(\frac{3}{2}^+ \otimes 1^-)_{\frac{3}{2}} \otimes 1^-$	$\frac{1}{15} (28\mu_u + 5\mu_c + 15\mu_{l(\Sigma_c^* + \bar{D}^0)})$	4.002
	$^6P_{\frac{5}{2}}$	$(\frac{3}{2}^+ \otimes 1^-)_{\frac{5}{2}} \otimes 1^-$	$\frac{1}{35} (93\mu_u + 10\mu_{l(\Sigma_c^{*++} + \bar{D}^0)})$	5.130
$\frac{7}{2}^+$	$^6P_{\frac{7}{2}}$	$\frac{3}{2}^+ \otimes 1^- \otimes 1^-$	$3\mu_u + \mu_{l(\Sigma_c^{*++} + \bar{D}^0)}$	6.015

Decays,” Phys. Rev. Lett. **115**, 072001 (2015).

- [16] R. Aaij *et al.* [LHCb], “Observation of $B_{(s)}^0 \rightarrow J/\psi p \bar{p}$ decays and precision measurements of the $B_{(s)}^0$ masses,” Phys. Rev. Lett. **122**, no.19, 191804 (2019).
- [17] T. Gershon [LHCb], “Exotic hadron naming convention,” [arXiv:2206.15233 [hep-ex]].
- [18] R. Aaij *et al.* [LHCb], “Evidence of a $J/\psi\Lambda$ structure and observation of excited Ξ^- states in the $\Xi_b^- \rightarrow J/\psi\Lambda K^-$ decay,” Sci. Bull. **66**, 1278-1287 (2021).
- [19] R. Aaij *et al.* [LHCb], “Evidence for a new structure in

the $J/\psi p$ and $J/\psi \bar{p}$ systems in $B_s^0 \rightarrow J/\psi p \bar{p}$ decays,” Phys. Rev. Lett. **128**, no.6, 062001 (2022).

- [20] [LHCb], “Observation of a $J/\psi\Lambda$ resonance consistent with a strange pentaquark candidate in $B^- \rightarrow J/\psi\Lambda \bar{p}$ decays,” [arXiv:2210.10346 [hep-ex]].
- [21] J. He, “Study of $P_c(4457)$, $P_c(4440)$, and $P_c(4312)$ in a quasipotential Bethe-Salpeter equation approach,” Eur. Phys. J. C **79**, no.5, 393 (2019).
- [22] M. Karliner and J. L. Rosner, “New Exotic Meson and Baryon Resonances from Doubly-Heavy Hadronic

TABLE XVII: The magnetic moments of the $P_\psi^{\Delta^-}$ states in the molecular model with the 10_f flavor representation. The $J_1^{P_1} \otimes J_2^{P_2} \otimes J_3^{P_3}$ are corresponding to the angular momentum and parity of baryon, meson and orbital, respectively. The $\mu_{l(\text{baryon/meson})}$ represents the orbital excitation between corresponding hadrons. The unit is the nuclear magnetic moment μ_N .

$ \Sigma_c^{(*)0} D^{(*)-}\rangle$				
J^P	$2s+1L_J$	$J_1^{P_1} \otimes J_2^{P_2} \otimes J_3^{P_3}$	Expressions	Results
$\frac{1}{2}^-$	$2S_{\frac{1}{2}}$	$\frac{1}{2}^+ \otimes 0^- \otimes 0^+$	$\frac{1}{3}(4\mu_d - \mu_c)$	-1.398
		$\frac{1}{2}^+ \otimes 1^- \otimes 0^+$	$\frac{1}{9}(2\mu_d - 5\mu_c)$	-0.435
		$\frac{3}{2}^+ \otimes 1^- \otimes 0^+$	$\frac{1}{9}(7\mu_d - 8\mu_c)$	-0.378
$\frac{3}{2}^-$	$4S_{\frac{3}{2}}$	$\frac{1}{2}^+ \otimes 1^- \otimes 0^+$	$\frac{1}{3}(7\mu_d - 4\mu_c)$	-2.749
		$\frac{3}{2}^+ \otimes 0^- \otimes 0^+$	$2\mu_d + \mu_c$	-1.492
		$\frac{3}{2}^+ \otimes 1^- \otimes 0^+$	$\frac{1}{15}(28\mu_d + 5\mu_c)$	-1.634
$\frac{5}{2}^-$	$6S_{\frac{5}{2}}$	$\frac{3}{2}^+ \otimes 1^- \otimes 0^+$	$3\mu_d$	-2.842
$\frac{1}{2}^+$	$2P_{\frac{1}{2}}$	$\frac{1}{2}^+ \otimes 0^- \otimes 1^-$	$\frac{1}{9}(-4\mu_d + \mu_c + 6\mu_{l(\Sigma_c^0/D^-)})$	0.276
		$(\frac{1}{2}^+ \otimes 1^-)_{\frac{1}{2}} \otimes 1^-$	$\frac{1}{27}(-2\mu_d + 5\mu_c + 18\mu_{l(\Sigma_c^0/D^{*-})})$	0.316
	$4P_{\frac{1}{2}}$	$(\frac{1}{2}^+ \otimes 1^-)_{\frac{3}{2}} \otimes 1^-$	$\frac{1}{27}(35\mu_d - 20\mu_c - 9\mu_{l(\Sigma_c^0/D^{*-})})$	-1.442
		$\frac{3}{2}^+ \otimes 0^- \otimes 1^-$	$\frac{1}{9}(10\mu_d + 5\mu_c - 3\mu_{l(\Sigma_c^{*0}/D^-)})$	-0.733
	$2P_{\frac{1}{2}}$	$(\frac{3}{2}^+ \otimes 1^-)_{\frac{1}{2}} \otimes 1^-$	$\frac{1}{27}(-7\mu_d - 8\mu_c + 18\mu_{l(\Sigma_c^{*0}/D^{*-})})$	-0.047
	$4P_{\frac{1}{2}}$	$(\frac{3}{2}^+ \otimes 1^-)_{\frac{3}{2}} \otimes 1^-$	$\frac{1}{27}(28\mu_d + 5\mu_c - 9\mu_{l(\Sigma_c^{*0}/D^{*-})})$	-0.821
$\frac{3}{2}^+$	$2P_{\frac{3}{2}}$	$\frac{1}{2}^+ \otimes 0^- \otimes 1^-$	$\frac{1}{3}(4\mu_d - \mu_c + 3\mu_{l(\Sigma_c^0/D^-)})$	-1.682
		$(\frac{1}{2}^+ \otimes 1^-)_{\frac{1}{2}} \otimes 1^-$	$\frac{1}{9}(2\mu_d - 5\mu_c + 9\mu_{l(\Sigma_c^0/D^{*-})})$	-0.691
	$4P_{\frac{3}{2}}$	$(\frac{1}{2}^+ \otimes 1^-)_{\frac{3}{2}} \otimes 1^-$	$\frac{1}{45}(77\mu_d - 44\mu_c + 18\mu_{l(\Sigma_c^0/D^{*-})})$	-2.118
		$\frac{3}{2}^+ \otimes 0^- \otimes 1^-$	$\frac{1}{15}(22\mu_d + 11\mu_c + 6\mu_{l(\Sigma_c^{*0}/D^-)})$	-1.209
	$2P_{\frac{3}{2}}$	$(\frac{3}{2}^+ \otimes 1^-)_{\frac{1}{2}} \otimes 1^-$	$\frac{1}{9}(7\mu_d + 8\mu_c + 9\mu_{l(\Sigma_c^{*0}/D^{*-})})$	-0.638
	$4P_{\frac{3}{2}}$	$(\frac{3}{2}^+ \otimes 1^-)_{\frac{3}{2}} \otimes 1^-$	$\frac{1}{225}(308\mu_d + 55\mu_c + 90\mu_{l(\Sigma_c^{*0}/D^{*-})})$	-1.302
$6P_{\frac{3}{2}}$	$(\frac{3}{2}^+ \otimes 1^-)_{\frac{5}{2}} \otimes 1^-$	$\frac{1}{25}(63\mu_d - 15\mu_{l(\Sigma_c^{*0}/D^{*-})})$	-2.232	
$\frac{5}{2}^+$	$4P_{\frac{5}{2}}$	$\frac{1}{2}^+ \otimes 1^- \otimes 1^-$	$\frac{1}{3}(7\mu_d - 4\mu_c + 3\mu_{l(\Sigma_c^+/D^{*0})})$	-3.005
		$\frac{3}{2}^+ \otimes 0^- \otimes 1^-$	$2\mu_d + \mu_c + \mu_{l(\Sigma_c^{*0}/D^-)}$	-1.779
		$(\frac{3}{2}^+ \otimes 1^-)_{\frac{3}{2}} \otimes 1^-$	$\frac{1}{15}(28\mu_d + 5\mu_c + 15\mu_{l(\Sigma_c^{*0}/D^{*-})})$	-1.894
	$6P_{\frac{5}{2}}$	$(\frac{3}{2}^+ \otimes 1^-)_{\frac{5}{2}} \otimes 1^-$	$\frac{1}{35}(93\mu_d + 10\mu_{l(\Sigma_c^{*0}/D^{*-})})$	-2.592
$\frac{7}{2}^+$	$6P_{\frac{7}{2}}$	$\frac{3}{2}^+ \otimes 1^- \otimes 1^-$	$3\mu_d + \mu_{l(\Sigma_c^{*0}/D^{*-})}$	-3.102

Molecules,” Phys. Rev. Lett. **115**, no.12, 122001 (2015).

- [23] T. J. Burns, “Phenomenology of $P_c(4380)^+$, $P_c(4450)^+$ and related states,” Eur. Phys. J. A **51**, no.11, 152 (2015).
- [24] M. Monemzadeh, N. Tazimiand and S. Babaghorat, “Calculating Masses of Pentaquarks Composed of Baryons and Mesons,” Adv. High Energy Phys. **2016**, 6480926 (2016).
- [25] G. Yang and J. Ping, “The structure of pentaquarks P_c^+ in the chiral quark model,” Phys. Rev. D **95**, no.1, 014010

(2017).

- [26] H. Huang, C. Deng, J. Ping and F. Wang, “Possible pentaquarks with heavy quarks,” Eur. Phys. J. C **76**, no.11, 624 (2016).
- [27] Y. Shimizu, Y. Yamaguchi and M. Harada, “Heavy quark spin multiplet structure of $P_c(4312)$, $P_c(4440)$, and $P_c(4457)$,” [arXiv:1904.00587 [hep-ph]].
- [28] H. X. Chen, W. Chen, X. Liu, T. G. Steele and S. L. Zhu, “Towards exotic hidden-charm pentaquarks in QCD,” Phys. Rev. Lett. **115**, no.17, 172001 (2015).

TABLE XVIII: Transition magnetic moments between the S -wave $\Sigma_c^{(*)}\bar{D}^{(*)}$ -type hidden-charm molecular pentaquarks $P_\psi^{\Delta^{++}}$ with 10_f flavor representation. The unit is the nuclear magnetic moment μ_N .

Decay modes	Expressions	Results
$\Sigma_c\bar{D}^* \frac{1}{2}^-\rangle \rightarrow \Sigma_c\bar{D} \frac{1}{2}^-\rangle\gamma$	$\frac{\sqrt{3}}{3}\mu_{\bar{D}^{*0}\rightarrow\bar{D}^0}$	-1.327
$\Sigma_c\bar{D}^* \frac{3}{2}^-\rangle \rightarrow \Sigma_c\bar{D} \frac{1}{2}^-\rangle\gamma$	$\frac{\sqrt{6}}{3}\mu_{\bar{D}^{*0}\rightarrow\bar{D}^0}$	-1.877
$\Sigma_c\bar{D}^* \frac{3}{2}^-\rangle \rightarrow \Sigma_c\bar{D}^* \frac{1}{2}^-\rangle\gamma$	$\frac{\sqrt{2}}{3}(2\mu_{\Sigma_c^{++}} - \mu_{\bar{D}^{*0}})$	1.552
$\Sigma_c^*\bar{D}^* \frac{1}{2}^-\rangle \rightarrow \Sigma_c\bar{D}^* \frac{3}{2}^-\rangle\gamma$	$-\frac{\sqrt{2}}{2}\mu_{\Sigma_c^{*++}\rightarrow\Sigma_c^{++}}$	-0.994
$\Sigma_c^*\bar{D} \frac{3}{2}^-\rangle \rightarrow \Sigma_c\bar{D} \frac{1}{2}^-\rangle\gamma$	$\mu_{\Sigma_c^{*++}\rightarrow\Sigma_c^{++}}$	1.406
$\Sigma_c^*\bar{D}^* \frac{1}{2}^-\rangle \rightarrow \Sigma_c^*\bar{D} \frac{3}{2}^-\rangle\gamma$	$-\frac{\sqrt{3}}{3}\mu_{\bar{D}^{*0}\rightarrow\bar{D}^0}$	1.327
$\Sigma_c^*\bar{D}^* \frac{3}{2}^-\rangle \rightarrow \Sigma_c\bar{D}^* \frac{1}{2}^-\rangle\gamma$	$-\frac{\sqrt{5}}{5}\mu_{\Sigma_c^{*++}\rightarrow\Sigma_c^{++}}$	-0.629
$\Sigma_c^*\bar{D}^* \frac{3}{2}^-\rangle \rightarrow \Sigma_c^*\bar{D}^* \frac{1}{2}^-\rangle\gamma$	$\frac{\sqrt{5}}{25}(2\mu_{\Sigma_c^{*++}} - 3\mu_{\bar{D}^{*0}})$	0.028
$\Sigma_c^*\bar{D}^* \frac{3}{2}^-\rangle \rightarrow \Sigma_c\bar{D}^* \frac{3}{2}^-\rangle\gamma$	$-\frac{\sqrt{10}}{5}\mu_{\Sigma_c^{*++}\rightarrow\Sigma_c^{++}}$	-0.889
$\Sigma_c^*\bar{D}^* \frac{3}{2}^-\rangle \rightarrow \Sigma_c^*\bar{D} \frac{3}{2}^-\rangle\gamma$	$\frac{\sqrt{15}}{5}\mu_{\bar{D}^{*0}\rightarrow\bar{D}^0}$	-1.780
$\Sigma_c^*\bar{D}^* \frac{5}{2}^-\rangle \rightarrow \Sigma_c\bar{D}^* \frac{1}{2}^-\rangle\gamma$	$\frac{2\sqrt{5}}{5}\mu_{\Sigma_c^{*++}\rightarrow\Sigma_c^{++}}$	1.258
$\Sigma_c^*\bar{D}^* \frac{5}{2}^-\rangle \rightarrow \Sigma_c^*\bar{D} \frac{3}{2}^-\rangle\gamma$	$\frac{\sqrt{10}}{5}\mu_{\bar{D}^{*0}\rightarrow\bar{D}^0}$	-1.454
$\Sigma_c^*\bar{D}^* \frac{5}{2}^-\rangle \rightarrow \Sigma_c\bar{D}^* \frac{3}{2}^-\rangle\gamma$	$\frac{\sqrt{15}}{5}\mu_{\Sigma_c^{*++}\rightarrow\Sigma_c^{++}}$	1.089
$\Sigma_c^*\bar{D}^* \frac{5}{2}^-\rangle \rightarrow \Sigma_c^*\bar{D}^* \frac{3}{2}^-\rangle\gamma$	$\frac{\sqrt{6}}{15}(2\mu_{\Sigma_c^{*++}} - 3\mu_{\bar{D}^{*0}})$	0.051

- [29] R. Chen, X. Liu and S. L. Zhu, “Hidden-charm molecular pentaquarks and their charm-strange partners,” Nucl. Phys. A **954**, 406-421 (2016).
- [30] S. X. Nakamura, A. Hosaka and Y. Yamaguchi, “ $P_c(4312)^+$ and $P_c(4337)^+$ as interfering $\Sigma_c\bar{D}$ and $\Lambda_c\bar{D}^*$ threshold cusps,” Phys. Rev. D **104**, no.9, L091503 (2021).
- [31] X. Z. Ling, J. X. Lu, M. Z. Liu and L. S. Geng, “ $P_c(4457) \rightarrow P_c(4312)\pi/\gamma$ in the molecular picture,” Phys. Rev. D **104**, no.7, 074022 (2021).
- [32] L. Maiani, A. D. Polosa and V. Riquer, “The New Pentaquarks in the Diquark Model,” Phys. Lett. B **749**, 289-291 (2015).
- [33] G. N. Li, X. G. He and M. He, “Some Predictions of Diquark Model for Hidden Charm Pentaquark Discovered at the LHCb,” JHEP **12**, 128 (2015).
- [34] Z. G. Wang, “Analysis of $P_c(4380)$ and $P_c(4450)$ as pentaquark states in the diquark model with QCD sum rules,” Eur. Phys. J. C **76**, no.2, 70 (2016).
- [35] V. V. Anisovich, M. A. Matveev, J. Nyiri, A. V. Sarantsev and A. N. Semenova, “Pentaquarks and resonances in the pJ/ψ spectrum,” [arXiv:1507.07652 [hep-ph]].
- [36] P. P. Shi, F. Huang and W. L. Wang, “Hidden charm pentaquark states in a diquark model,” Eur. Phys. J. A **57**, no.7, 237 (2021).
- [37] A. Ali, I. Ahmed, M. J. Aslam, A. Parkhomenko and A. Rehman, “Interpretation of LHCb Hidden-Charm Pentaquarks within the Compact Diquark Model,” PoS **ICHEP2020**, 527 (2021).
- [38] Z. G. Wang, “Analysis of the $P_{cs}(4459)$ as the hidden-charm pentaquark state with QCD sum rules,” Int. J. Mod. Phys. A **36**, no.10, 2150071 (2021).
- [39] R. F. Lebed, “The Pentaquark Candidates in the Dynamical Diquark Picture,” Phys. Lett. B **749**, 454-457 (2015).
- [40] R. Zhu and C. F. Qiao, “Pentaquark states in a diquark-triquark model,” Phys. Lett. B **756**, 259-264 (2016).
- [41] J. F. Giron, R. F. Lebed and S. R. Martinez, “Spectrum of hidden-charm, open-strange exotics in the dynamical diquark model,” Phys. Rev. D **104**, no.5, 054001 (2021).
- [42] M. I. Eides, V. Y. Petrov and M. V. Polyakov, “New

TABLE XIX: Transition magnetic moments between the S -wave $\Sigma_c^{(*)}D^{(*)}$ -type hidden-charm molecular pentaquarks $P_\psi^{\Delta^-}$ with 10_f flavor representation. The unit is the nuclear magnetic moment μ_N .

Decay modes	Expressions	Results
$\Sigma_c D^* \frac{1}{2}^- \rangle \rightarrow \Sigma_c D \frac{1}{2}^- \rangle \gamma$	$\frac{\sqrt{3}}{3} \mu_{D^{*-} \rightarrow D^-}$	0.314
$\Sigma_c D^* \frac{3}{2}^- \rangle \rightarrow \Sigma_c D \frac{1}{2}^- \rangle \gamma$	$\frac{\sqrt{6}}{3} \mu_{D^{*-} \rightarrow D^-}$	0.444
$\Sigma_c D^* \frac{3}{2}^- \rangle \rightarrow \Sigma_c D^* \frac{1}{2}^- \rangle \gamma$	$\frac{\sqrt{2}}{3} (2\mu_{\Sigma_c^0} - \mu_{D^{*-}})$	-0.681
$\Sigma_c^* D^* \frac{1}{2}^- \rangle \rightarrow \Sigma_c D^* \frac{3}{2}^- \rangle \gamma$	$-\frac{\sqrt{2}}{2} \mu_{\Sigma_c^{*0} \rightarrow \Sigma_c^0}$	0.901
$\Sigma_c^* D \frac{3}{2}^- \rangle \rightarrow \Sigma_c D \frac{1}{2}^- \rangle \gamma$	$\mu_{\Sigma_c^{*0} \rightarrow \Sigma_c^0}$	-1.273
$\Sigma_c^* D^* \frac{1}{2}^- \rangle \rightarrow \Sigma_c^* D \frac{3}{2}^- \rangle \gamma$	$-\frac{\sqrt{3}}{3} \mu_{D^{*-} \rightarrow D^-}$	-0.314
$\Sigma_c^* D^* \frac{3}{2}^- \rangle \rightarrow \Sigma_c D^* \frac{1}{2}^- \rangle \gamma$	$-\frac{\sqrt{5}}{5} \mu_{\Sigma_c^{*0} \rightarrow \Sigma_c^0}$	0.570
$\Sigma_c^* D^* \frac{3}{2}^- \rangle \rightarrow \Sigma_c^* D^* \frac{1}{2}^- \rangle \gamma$	$\frac{\sqrt{5}}{25} (2\mu_{\Sigma_c^{*0}} - 3\mu_{D^{*-}})$	0.112
$\Sigma_c^* D^* \frac{3}{2}^- \rangle \rightarrow \Sigma_c D^* \frac{3}{2}^- \rangle \gamma$	$-\frac{\sqrt{10}}{5} \mu_{\Sigma_c^{*0} \rightarrow \Sigma_c^0}$	0.806
$\Sigma_c^* D^* \frac{3}{2}^- \rangle \rightarrow \Sigma_c^* D \frac{3}{2}^- \rangle \gamma$	$\frac{\sqrt{15}}{5} \mu_{D^{*-} \rightarrow D^-}$	0.421
$\Sigma_c^* D^* \frac{5}{2}^- \rangle \rightarrow \Sigma_c D^* \frac{1}{2}^- \rangle \gamma$	$\frac{2\sqrt{5}}{5} \mu_{\Sigma_c^{*0} \rightarrow \Sigma_c^0}$	-1.139
$\Sigma_c^* D^* \frac{5}{2}^- \rangle \rightarrow \Sigma_c^* D \frac{3}{2}^- \rangle \gamma$	$\frac{\sqrt{10}}{5} \mu_{D^{*-} \rightarrow D^-}$	0.344
$\Sigma_c^* D^* \frac{5}{2}^- \rangle \rightarrow \Sigma_c D^* \frac{3}{2}^- \rangle \gamma$	$\frac{\sqrt{15}}{5} \mu_{\Sigma_c^{*0} \rightarrow \Sigma_c^0}$	-0.987
$\Sigma_c^* D^* \frac{5}{2}^- \rangle \rightarrow \Sigma_c^* D^* \frac{3}{2}^- \rangle \gamma$	$\frac{\sqrt{6}}{15} (2\mu_{\Sigma_c^{*0}} - 3\mu_{D^{*-}})$	0.205

LHCb pentaquarks as hadrocharmonium states,” Mod. Phys. Lett. A **35**, no.18, 2050151 (2020).

- [43] C. Fernández-Ramírez *et al.* [JPAC], “Interpretation of the LHCb $P_c(4312)^+$ Signal,” Phys. Rev. Lett. **123**, no.9, 092001 (2019).
- [44] S. X. Nakamura, “ $P_c(4312)^+$, $P_c(4380)^+$, and $P_c(4457)^+$ as double triangle cusps,” Phys. Rev. D **103**, 111503 (2021).
- [45] Z. Y. Yang, F. Z. Peng, M. J. Yan, M. Sánchez Sánchez and M. Pavon Valderrama, “Molecular P_ψ pentaquarks from light-meson exchange saturation,” [arXiv:2211.08211 [hep-ph]].
- [46] J. T. Zhu, S. Y. Kong and J. He, “ $P_{\psi_s}^\Lambda(4459)$ and $P_{\psi_s}^\Lambda(4338)$ as molecular states in $J/\psi\Lambda$ invariant mass spectra,” [arXiv:2211.06232 [hep-ph]].
- [47] X. Z. Weng, X. L. Chen, W. Z. Deng and S. L. Zhu, “Hidden-charm pentaquarks and P_c states,” Phys. Rev. D **100**, no.1, 016014 (2019).
- [48] F. L. Wang, H. Y. Zhou, Z. W. Liu and X. Liu, “What can we learn from the electromagnetic properties of hidden-charm molecular pentaquarks with single strangeness?,” Phys. Rev. D **106**, no.5, 054020 (2022).
- [49] H. Y. Zhou, F. L. Wang, Z. W. Liu and X. Liu, “Probing the electromagnetic properties of the $\Sigma_c^{(*)}D^{(*)}$ -type doubly charmed molecular pentaquarks,” Phys. Rev. D **106**, no.3, 034034 (2022).
- [50] W. X. Zhang, H. Xu and D. Jia, “Masses and magnetic moments of hadrons with one and two open heavy quarks: Heavy baryons and tetraquarks,” Phys. Rev. D **104**, no.11, 114011 (2021).
- [51] G. J. Wang, R. Chen, L. Ma, X. Liu and S. L. Zhu, “Magnetic moments of the hidden-charm pentaquark states,” Phys. Rev. D **94**, no.9, 094018 (2016).
- [52] M. W. Li, Z. W. Liu, Z. F. Sun and R. Chen, “Magnetic moments and transition magnetic moments of P_c and P_{cs} states,” Phys. Rev. D **104**, no.5, 054016 (2021).
- [53] F. Gao and H. S. Li, “Magnetic moments of hidden-charm strange pentaquark states*,” Chin. Phys. C **46**, no.12, 123111 (2022).
- [54] F. L. Wang, H. Y. Zhou, Z. W. Liu and X. Liu, “Exploring the electromagnetic properties of the $\Xi_c^{(\prime,*)}\bar{D}_s^*$ and $\Omega_c^{(*)}\bar{D}_s^*$ molecular states,” [arXiv:2210.02809 [hep-ph]].

- [55] B. Wang, B. Yang, L. Meng and S. L. Zhu, “Radiative transitions and magnetic moments of the charmed and bottom vector mesons in chiral perturbation theory,” *Phys. Rev. D* **100**, no.1, 016019 (2019).
- [56] E. Ortiz-Pacheco, R. Bijker and C. Fernández-Ramírez, “Hidden charm pentaquarks: mass spectrum, magnetic moments, and photocouplings,” *J. Phys. G* **46**, no.6, 065104 (2019).
- [57] Y. R. Liu, P. Z. Huang, W. Z. Deng, X. L. Chen and S. L. Zhu, “Pentaquark magnetic moments in different models,” *Phys. Rev. C* **69**, 035205 (2004).
- [58] U. Özdem, “Investigation of magnetic moment of $P_{cs}(4338)$ and $P_{cs}(4459)$ pentaquark states,” *Phys. Lett. B* **836**, 137635 (2023).
- [59] U. Özdem, “Magnetic dipole moments of the hidden-charm pentaquark states: $P_c(4440)$, $P_c(4457)$ and $P_{cs}(4459)$,” *Eur. Phys. J. C* **81**, no.4, 277 (2021).
- [60] U. Özdem, “Magnetic moments of pentaquark states in light-cone sum rules,” *Eur. Phys. J. A* **58**, no.3, 46 (2022).
- [61] U. Özdem, “Electromagnetic properties of doubly heavy pentaquark states,” *Eur. Phys. J. Plus* **137**, 936 (2022).
- [62] R. L. Workman *et al.* [Particle Data Group], “Review of Particle Physics,” *PTEP* **2022**, 083C01 (2022).
- [63] J. Jiang, S. Z. Jiang, S. Y. Li, Y. R. Liu, Z. G. Si and H. Q. Wang, “Relations for low-energy constants in baryon chiral perturbation theory with explicit $\Delta(1232)$ derived from the chiral quark model,” *Eur. Phys. J. C* **83**, no.4, 296 (2023).
- [64] D. Ebert, R. N. Faustov and V. O. Galkin, “Masses of tetraquarks with open charm and bottom,” *Phys. Lett. B* **696**, 241-245 (2011).